AD-A128 100 SIMULTANEOUS PROCESSING OF PHOTOGRAPHIC AND ACCELEROMETER ARRAY DATA FROM..(U) CHARLES STARK DRAPER LAB INC CAMBRIDGE MA M E ASH DEC 82 AFAMRL-TR-82-73 1/1

UNCLASSIFIED F33615-76-C-0520 F/G 6/19 NL

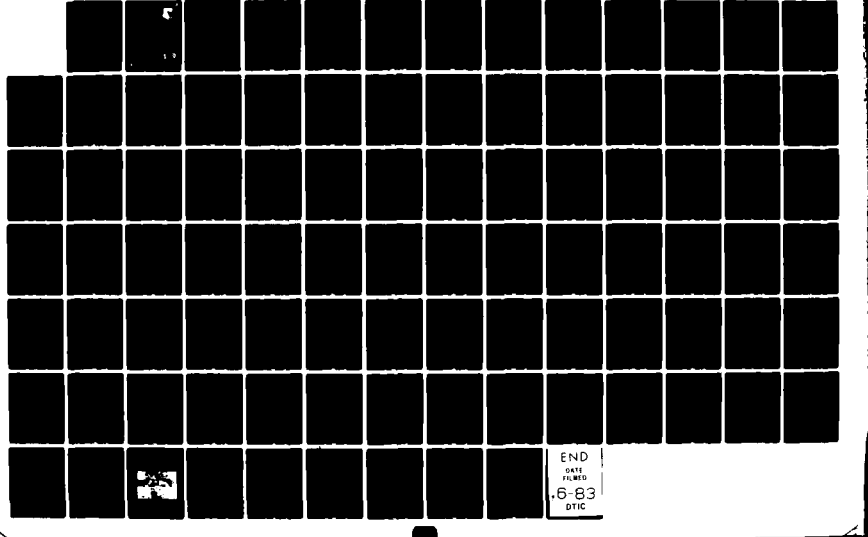

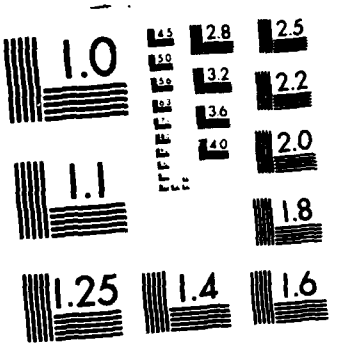

[illegible] PROCESSING OF PHOTOGRAPHIC [illegible] ARRAY DATA FROM SLED IMPACT EXPERIMENTS

MICHAEL E. ASH
THE CHARLES STARK DRAPER LABORATORY, INC.
555 TECHNOLOGY SQUARE
CAMBRIDGE, MA 02139

[illegible] 1982

[redacted] drawings, specifications, or other data are used for any purpose other than a [redacted] connection with a definitely Government procurement operation, the Government thereby incurs no responsibility nor any obligation whatsoever; and the fact that the Government may have formulated, furnished, or in any way supplied the said drawings, specifications, or other data, is not to be regarded by implication or otherwise, or in any manner licensing the holder or any other person or corporation, or conveying any rights or permission to manufacture, use, or sell any patented invention that may in any way be related thereto.

Please do not request copies of this report from Air Force Aerospace Medical Research Laboratory. Additional copies may be purchased from:

National Technical Information Service
5285 Port Royal Road
Springfield, Virginia 22161

Federal Government agencies and their contractors registered with Defense Technical Information Center should direct requests for copies of this report to:

Defense Technical Information Center
Cameron Station
Alexandria, Virginia 22314

TECHNICAL REVIEW AND APPROVAL

AFAMRL-TR-82-73

This report has been reviewed by the Office of Public Affairs (PA) and is releasable to the National Technical Information Service (NTIS). At NTIS, it will be available to the general public, including foreign nations.

This technical report has been reviewed and is approved for publication.

[redacted]

SECURITY CLASSIFICATION OF THIS PAGE *(When Data Entered)*

REPORT DOCUMENTATION PAGE

READ INSTRUCTIONS BEFORE COMPLETING FORM

1. REPORT NUMBER: AFAMRL-TR-82-73
2. GOVT ACCESSION NO.: AD-A128 107
3. RECIPIENT'S CATALOG NUMBER:

4. TITLE *(and Subtitle)*: Simultaneous Processing of Photographic and Accelerometer Array Data from Sled Impact Experiments

5. TYPE OF REPORT & PERIOD COVERED:

6. PERFORMING ORG. REPORT NUMBER:

7. AUTHOR(s): Michael E. Ash

8. CONTRACT OR GRANT NUMBER(s): F33615-76-C-0520

9. PERFORMING ORGANIZATION NAME AND ADDRESS: The Charles Stark Draper Laboratory, Inc. 555 Technology Square, Cambridge, MA 02139

10. PROGRAM ELEMENT, PROJECT, TASK AREA & WORK UNIT NUMBERS: 62202F/7231/16/18

11. CONTROLLING OFFICE NAME AND ADDRESS: Biomechanical Protection Branch, Biodynamics & Bioengineering Division, Air Force Aerospace Medical Research Laboratory, Wright-Patterson Air Force Base, Ohio 45433

12. REPORT DATE: December 1982

13. NUMBER OF PAGES: 91

14. MONITORING AGENCY NAME & ADDRESS *(if different from Controlling Office)*:

15. SECURITY CLASS. *(of this report)*: Unclassified

15a. DECLASSIFICATION/DOWNGRADING SCHEDULE:

16. DISTRIBUTION STATEMENT *(of this Report)*

Approved for public release; distribution unlimited.

17. DISTRIBUTION STATEMENT *(of the abstract entered in Block 20, if different from Report)*

18. SUPPLEMENTARY NOTES

PROJECT MONITOR - JAMES W. BRINKLEY, 53931

19. KEY WORDS *(Continue on reverse side if necessary and identify by block number)*

Accelerometer Array
Kalman Filter
Biodynamics
Biomechanics
Impact Experiment
Quaternion

20. ABSTRACT *(Continue on reverse side if necessary and identify by block number)*

A Quaternion-Kalman filter model is derived to simultaneously analyze accelerometer array and photographic data from sled impact experiments. Formulas are given for the quaternion representation of rotations, the propagation of dynamical states and their partial derivatives, the observables and their partial derivatives, and the Kalman filter update of the state given the observables. The observables are accelerometer and tachometer velocity data of the sled relative to the track, linear accelerometer array and photographic data of the subject relative to the sled, and ideal angular accelerometer data. The quaternion-

DD FORM 1 JAN 73 1473 EDITION OF 1 NOV 65 IS OBSOLETE

SECURITY CLASSIFICATION OF THIS PAGE *(When Data Entered)*

BLOCK 20 (continued)
constraints enter through perfect constraint observations and normalization after a state update. Lateral and fore-aft impact tests are analyzed with Fortran IV software written using the formulas of this report.

PREFACE

This report was prepared by The Charles Stark Draper Laboratory, Inc. under subcontract from Dynalectron Corporation, Scientific Services Division, in performance of Air Force Contract F33615-76-C-0520 for the Biomechanical Protection Branch of the Biodynamics and Bioengineering Division, Air Force Aerospace Medical Research Laboratory, Wright-Patterson Air Force Base, Ohio.

The Principal Investigator for The Charles Stark Draper Laboratory, Inc. was Dr. Michael Ash. The Supervising Engineer for Dynalectron Corporation was Mr. Harold Boedeker. The Air Force Technical Monitor was Mr. James W. Brinkley of the Biomechanical Protection Branch, Biodynamics and Bioengineering Division. Special technical assistance was provided by Lt Col James Raddin, Jr., M.D., of the Biomechanical Protection Branch, Biodynamics and Bioengineering Division.

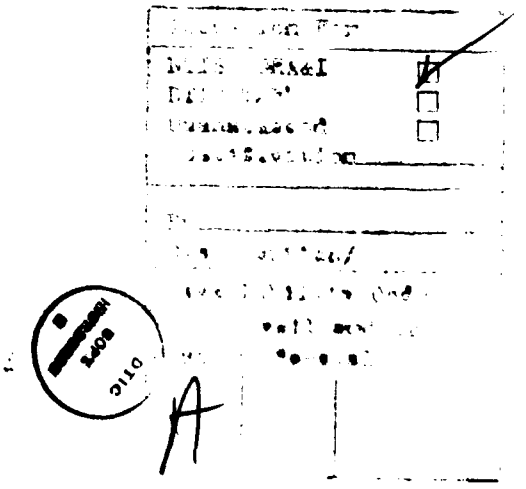

TABLE OF CONTENTS

TABLE OF CONTENTS (Continued)

LIST OF FIGURES

LIST OF TABLES

NOTATION

a	=	(a_1, a_2, a_3, a_4)	quaternion
A	=	(A_{ij})	3 dimensional orthogonal transformation matrix
A			24 x 24 matrix multiplying states in linear dynamical differential equations
A_{3x3}			3 x 3 submatrix of A for y states
A_{9x9}			9 x 9 submatrix of A for z states
A_{12x12}			12 x 12 submatrix of A for $\bar{q}$ states
b	=	(b_1, b_2, b_3, b_4)	quaternion
b_i	=	$(0, b_{i1}, b_{i2}, b_{i3})$	quaternion defining position of accelerometer i relative to the center of the accelerometer array in accelerometer array frame
$\bar{\bar{b}}_i$	=	$(0, \bar{\bar{b}}_{i1}, \bar{\bar{b}}_{i2}, \bar{\bar{b}}_{i3})$	transform of b_i to the laboratory reference frame

NOTATION (continued)

c_i	$= (0, c_{i1}, c_{i2}, c_{i2})$	quaternion giving input axis direction of accelerometer i in accelerometer array frame
$\bar{c}_i$	$= (0, c_{i1}, c_{i2}, c_{i3})$	transform of c_i to the laboratory reference frame
d, d'		length of accelerometer array arms and offset of seismic masses from center lines of arms
D		diagonal scaling matrix
E		probability expectation operator
exp		matrix exponentiation
e_i	$= (0, e_{i1}, e_{i2}, e_{i3})$	fixed position coordinates of fiducial i relative to the accelerometer array frame
f_{0i}	$= (0, f_{0i1}, f_{0i2}, f_{0i3})$	initial position coordinates of fiducial i relative to sled frame
f_i	$= (0, f_{i1}, f_{i2}, f_{i3})$	position coordinates of fiducial i relative to sled frame at time t
$\vec{F}$		nonlinear state transition function
g		acceleration due to gravity (980.3 cm/s^2)
$\vec{H}$		nonlinear observables functions

NOTATION (continued)

I			Euler angle (angle between Z and Z' axes)
I			identity matrix in Kalman filter formulas
J			state Jacobian partial derivative matrix
K			Kalman filter gain matrix
L			observables Jacobian partial derivative matrix
M			general nonsymmetric matrix
P_f			state covariance matrix for forward Kalman filter
P_b			state covariance matrix for backward Kalman filter
P			state covariance matrix for Kalman smoother
$\bar{P}$			state covariance matrix before quaternion normalization
p	=	(p_1, p_2, p_3, p_4)	quaternion specify the rotation from the sled frame to the laboratory track frame (dimensionless)
q	=	(q_1, q_2, q_3, q_4)	quaternion specifying the rotational position of the accelerometer array frame relative to the sled frame (dimensionless)

NOTATION (continued)

(q_5, q_6, q_7, q_8)	quaternion specifying the rotational velocity of the accelerometer array frame relative to the sled frame (s^{-1})
$(q_9, q_{10}, q_{11}, q_{12})$	quaternion specifying the rotational acceleration of the accelerometer array frame relative to the sled frame (s^{-2})
$(\bar{q}_1, \ldots, \bar{q}_{12})$	$(q_1, \ldots, q_{12})$ before normalization
$Q = (Q_{ij})$	covariance matrix of $\vec{W}$ (integral of zero mean Gaussian white noise)
r	zero mean Gaussion noise in observation
R	covariance matrix of r
$\vec{r}$ (r)	body fixed vector (corresponding quaternion)
$\vec{s}$ (s)	body fixed vector (corresponding quaternion)
$\vec{s}$	observable vector $(\alpha_1, \ldots, \alpha_a, \beta_1, \ldots, \beta_b, \gamma_1, \gamma_2, \delta_1, \delta_2, \delta_3)^T$
S	general symmetrix matrix
t	time (seconds)
$t_0 = 0$	initial time (seconds)

NOTATION (continued)

t_k			time at kth step of Kalman filter-smoother (seconds)
T			superscript denoting matrix transpose
U			scaled symmetric matrix
v	=	$(0, v_1, v_2, v_3)$	quaternion with 0 real part (vector
$\vec{w}$	=	$(w_1, \ldots, w_{24})$	zero mean Gaussian white noise in the dynamics
$\vec{W}$			integral of zero mean Gaussian white noise $\vec{w}$
$\vec{x}$	=	$(x_1, \ldots, x_{24})$	state vector $(y_1, y_2, y_3, z_1, \ldots, z_9, q_1, \ldots, q_{24})$ resulting from Kalman smoother
$\vec{x}_f$			state vector resulting from Kalman forward filter
$\vec{x}_b$			state vector resulting from Kalman backward filter
$\vec{\bar{x}}$			state vector before quaternion normalization
(X, Y, Z)			accelerometer array reference system
$(\bar{X}, \bar{Y}, \bar{Z})$			sled reference system
$(\bar{\bar{X}}, \bar{\bar{Y}}, \bar{\bar{Z}})$			laboratory (track) reference system

NOTATION (continued)

y_1, y_2, y_3	translational position, velocity, and acceleration of the sled frame relative to the track frame (cm, cm/s, cm/s^2)
z_1, z_2, z_3	translational position of the accelerometer array frame relative to the sled frame (cm)
z_{10}, z_{20}, z_{30}	initial position of the accelerometer array frame relative to the sled frame (cm)
z_4, z_5, z_6	translational velocity of accelerometer array frame relative to the sled frame (cm/s)
z_7, z_8, z_9	translational acceleration of accelerometer array frame relative to the sled frame (cm/s^2)
α	real number
α_i	theoretical value of linear accelerometer i output (g), or angular accelerometer output (rad/s^2)
β_{ij}	theoretical value of photographic observable j of fiducial i (j = 1, 2, 3) (inches)
γ_1, γ_2	theoretical values of acceleration and velocity of sled relative to track observables (g, ft/s)

$\delta_1, \delta_2, \delta_3$		theoretical values of perfect quaternion constraint observables (dimensionless)
δ_{ij}		Kronecker delta
$\vec{\Delta}_j$		small adjustment to the state vector for checking partial derivatives by the difference method
$\delta\theta$		infinitesimal rotation angle
η_i	$= (0, \eta_{i1}, \eta_{i2}, \eta_{i3})$	specific acceleration quaternion of accelerometer i relative to the accelerometer array frame
θ		rotation angle
λ_a		*scale factor for accelerometer* observable (conversion from cm/s^2 to g = 1/980.3)
λ_b		scale factor for photographic observable (conversion from cm to inches = 2.54)
λ_c		scale factor for sled velocity observable (conversion from cm/s to ft/s = 1/(2.54 x 12))
μ_i		bias in linear accelerometer i output (value to be subtracted from measurement to yield specific acceleration) (g)

NOTATION (continued)

μ_{i0}			average value of accelerometer i output in its initial stationary orientation
ρ			length of a quaternion
ξ	=	$(0, \xi_1, \xi_2, \xi_3)$	angular acceleration quaternion in the accelerometer frame
Φ			linear state transition matrix
Ω			Euler angle
ω			Euler angle
ω	=	$(0, \omega_1, \omega_2, \omega_3)$	angular velocity quaternion in the *accelerometer reference frame*
$\overline{\overline{\omega}}$	=	$(0, \overline{\overline{\omega}}_1, \overline{\overline{\omega}}_2, \overline{\overline{\omega}}_3)$	angular velocity quaternion in the laboratory reference frame
$\overline{\omega}$	=	$(0, \overline{\omega}_1, \overline{\omega}_2, \overline{\omega}_3)$	angular velocity quaternion
$\vec{\omega}$	=	$(\omega_1, \omega_2, \omega_3)$	angular velocity vector

SECTION 1
INTRODUCTION

Human response to impact environments is investigated using instrumented anthropomorphic dummies, animal surrogates, cadavers, and human volunteers. This report addresses a new technique for analyzing the data from such experiments.

In a sled impact experiment, the dummy, animal, cadaver, or human subject is seated on a sled, which is given a sudden impetus down a track by a piston. Traditional observables used to analyze the resulting motion include accelerometer and tachometer velocity measurements of the motion of the sled relative to the track, photographic measurements of the motion of fiducials attached to the subject relative to the sled, and the output of linear piezoresistive accelerometers attached to the subject's body.

Because of the importance of separating translational and angular motions, linear accelerometer arrays are employed. However, small percentage errors in measuring a large linear accelerometer output could prove to be a large percentage error in the difference signal between two accelerometers, from which angular acceleration is derived. Thus, it is desirable to have light-weight instrumentation which can measure angular acceleration directly.

Even without angular accelerometers, improvements can be made in the traditional data analysis techniques. The accelerometer array data is currently analyzed separately from the photographic data, with the latter being used, at best, to provide an *ad hoc correction to the*

trajectory determined from the accelerometer array data. The more modern technique is to process all the data simultaneously through a Kalman filter to obtain the trajectory which best fits the accelerometer array, photographic, and sled accelerometer and tachometer velocity data.

The situation is analagous to navigating a cruise missile by simultaneously combining inertial instrument and external landmark sighting data. In the case of a sled impact experiment, the photographic camera fixed to the sled is looking at the subject, rather than on the vehicle looking at an external reference.

In order to simultaneously combine the various observables in a sled impact experiment, this report develops a quaternion-Kalman filter model of the motions in such an experiment, and analyzes actual experimental data with this technique. Head motion is particularly addressed. Covariance analyses are performed to investigate the possible accuracy improvement that could be obtained with an angular accelerometer. The Fortran computer program written to carry out this work is one of the deliverables of this contract.

1.1 ANALYSIS TECHNIQUE

Formulas are derived for the quaternion representation of the rotational motion of one reference frame relative to another, and for the corresponding angular velocity and acceleration. Unlike an Euler angle representation, the quaternion representation is valid for arbitrary angular motions, except that a constraint is required to restrict the four quaternion degrees of freedom to the three degrees of freedom existing in a rotation.

A state space dynamical system model is derived for an impact sled experiment. The state variables in units of centimeters, seconds, and radians are:

(a) Translational position, velocity, and acceleration of the sled frame relative to the track (three states);

(b) Translational position, velocity, and acceleration of an accelerometer array frame attached to the head relative to the sled frame (nine states); and

(c) Quaternion rotational position, velocity, and acceleration of the accelerometer array frame relative to the sled frame (12 states with 3 constraints).

The state dynamical equations are that the derivative of accleration (jerk) is equal to white noise.

Formulas are derived for photographic, tachometer, linear accelerometer, and ideal angular accelerometer observables in terms of the states, and for the partial derivatives of the observables with respect to the states. Kalman filter formulas are presented for the propagation of the state variables given the observables.

An experiment commences with the subject initially at rest with a small covariance for the uncertainty in its state initial conditions. The state is propagated to an observable time by the state dynamical equations. The state covariance is also so propagated, with the uncertainty being incremented by the white noise in the dynamics. This plant noise is a measure as to how much the acceleration can change between observable times, since the dynamical equations assume constant acceleration between observable times, except for the white noise. The state estimate and its covariance are updated using the observables and the Kalman filter formulas. The state is then propagated to the next observable time and the process repeated, etc.

The proper weighting of past states and present observables is determined by the relative size of the propagated state covariance and the covariance of the observables. Different observable types with their own units (g, inch, ft/s) can be combined, since the weighting covariance in the same units creates dimensionless combining terms.

The accelerometer observables are one millisecond apart, whereas the photographic observables are two milliseconds apart. There can be different numbers of observables at different observing times. In particular, if a sample-and-hold is not employed in a real time digital data acquisition system, then the slew in observable time for the analog-to-digital conversion of analog piezoresistive accelerometer data can be taken into account. The accelerometer measurements employed in this report were recorded on analog tape and played back for conversion to digital form, so the accelerometer data were at the same time.

The constraints on the quaternion state variables are taken into account in two ways. First, at each observation update time three additional perfect quaternion constraint observables for the rotational position, velocity, and acceleration are added to the real observables. These perfect constraint observables have zero error, and a form of the Kalman filter update formulas which allows zero observable covariance is employed. Second, after state propagation and observable updates, the quaternion states are normalized with the constraint conditions.

It was attempted to employ a Kalman smoother in fitting the trajectory to the observables, where the Kalman smoother estimate is the optimal combination of forward and backward Kalman filter estimates. The Kalman filter is propagated forward in time from the state initial conditions. Then the Kalman filter is run backwards from the last state estimate of the forward filter with completely uncertain covariance for this last point. It turned out that the backward filter did not thereby yield good state estimates, because the measurements at the first and subsequent time points into the past did not give complete observability into the states. Therefore, it is better to take presmoothed observables and run the forward Kalman filter starting with good initial conditions, rather than take raw observables and try to have the Kalman smoother get the smoothing effect of the past and future around each point.

Formulas are derived for both lateral and fore-aft (eyes out) impact sled tests. A quaternion rotation is required for the fore-aft orientation of the accelerometer array frame relative to the sled frame as compared to the orientation for the lateral case. The software implementing the quaternion-Kalman filter model formulas allows covariance analysis of simulated data as well as fitting to real data.

1.2 ANALYSIS SOFTWARE

Fortran IV software was written implementing the formulas of this report with extensive internal comments. The software was written, tested, and run on a large Amdahl (IBM 370-type) computer in such a way that it should be straightforward to convert it to run on a CDC 6600 computer at Wright-Patterson Air Force Base. Each subroutine commences with an

```
IMPLICIT REAL *8 (A-H, O-Z)
```

statement to force double precision 16 decimal place computations on the Amdahl computer. These statements would be removed or commented out on the CDC 6600 and single precision 14 decimal place computations employed. These and other statements which are expected to require change on a CDC 6600 are flagged by comment cards with asterisks.

A list of the 31 subroutines in the sled impact data analysis program is given in Table 1-1. There is a total of 3,107 lines of code, including comments. The memory required on the Amdahl computer is 268K bytes. This could be reduced to 200K bytes ≈ 30K CDC 6600 60 bit words using overlay.

A typical 300 millisecond impact Kalman filter run with data every millisecond (nine linear accelerometer array, six photographic fiducial coordinate, and sled accelerometer and tachometer observables) required 2.3 minutes of CPU time on the Amdahl computer, which would be somewhat greater on a CDC 6600 computer. Changes could be made to the software to make it slightly more efficient.

Table 1-1. Impact sled test Fortran subroutines.

Subroutine Name	Number of Lines	Description
AAMAIN	105	Main Program
ANGACL	126	Process Angular Accelerometer Observables
DOT	24	Calculate the Dot Product of Two 3 Vectors
DSTATE	81	Calculate State Transition Jacobian Partial Derivative Matrix
ERRWGT	78	Alter Individual Observation Errors Using Input Error Weights
FILTB	328	Backward Kalman Filter and Kalman Smoother
FILTF	274	Forward Kalman Filter
INPUT	547	Read Input Control Parameters for Given Experiment
KALCOV	66	Perform Kalman Filter State Covariance Update
KALGAN	46	Calculate Kalman Filter Gain Matrix
LINACL	196	Process Linear Accelerometer Observables
MATMLT	40	General Matrix Multiplication AB^T
MATMUL	40	General Matrix Multiplication AB
OBSERV	136	Process Observations, Including Quaternion Constraints
PHOTO	111	Process Photographic Fiducial Observables
PNOISE	62	Determine the State Dynamical Plant Noise
QAUTO	48	Quaternion Automorphism
QCONJ	25	Quaternion Conjugate
QNORMX	57	Normalize Quaternion Rotational Position, Velocity, Acceleration
QNPART	84	Quaternion Normalization Partial Derivatives
QPROD	27	Quaternion Product
QSTRNT	57	Apply Quaternion Constraint to State Vector and Its Covariance
SCLINV	71	Scale a Symmetric Matrix Before Calling Matrix Inversion

Table 1-1. Impact sled test Fortran subroutines. (Continued)

Subroutine Name	Number of Lines	Description
STATE	95	Propagate State and Calculate the State Transition Matrix
SYMADD	27	Symmetric Matrix Addition
SYMINV	104	Symmetric Matrix Inversion In Place
SZMUL	40	Matrix Multiplication SZ
TRACK	68	Process Motion Relative To Track Observables
ZSMUL	40	Matrix Multiplication ZS
ZSZMLT	55	Matrix Multiplication Z^TSZ
ZSZMUL	55	Matrix Multiplication ZSZ^T
Total	3,113	

Very extensive tests were performed on the software. The consistency of the state propagation equations and the Jacobian partial derivatives was checked by the difference method. The same technique was used for checking observable and partial derivative formulas for sled accelerometer and tachometer velocity observables, linear accelerometer and ideal angular accelerometer observables, photographic observables, and perfect quaternion constraint observables. Matrix manipulation subroutines were also checked. For example, the product of a matrix with its calculated inverse was compared with the identity matrix.

Successful checkout of the Kalman filter code was done once the correctness of these various service subroutines was verified. The ultimate test was that the Kalman filter tracked real data.

A plotting routine was written to display the results of data analyses. By its nature, such a program is installation specific, so an equivalent program would have to be specially written for the CDC

6600. Similarly, installation specific software was written to read magnetic and punched paper tapes containing impact sled test data; equivalent software would also be required on the CDC 6600.

1.3 FITS TO DATA

Two lateral and two fore-aft (eyes out) impact sled tests were analyzed with the Kalman filter software. There was a dummy and a human test for each given type of experiment.

Lightweight Endevco 2264-200 piezoresistive linear accelerometer arrays were employed. In the lateral impact case there was a nine-accelerometer array strapped to the side of the head, and in the fore-aft impact case, it was strapped to the front of the head. In the fore-aft experiment only three of the nine outputs were used to simulate the situation of a three-accelerometer array afixed to the teeth inside the mouth. This latter arrangement is starting to be used because the accelerometer array is thereby more firmly attached to the skull than when it is strapped to the head over the pliable skin.

In the lateral impact tests, the post-fit data residuals show that the Kalman filter is tracking the observables, which indicates that it is mathematically working. Some of the residuals are 20 to 30 percent of the size of the 10 g magnitude impact event. Slight changes in the input values of the coordinates and orientations of the fiducials and accelerometers relative to each other could cause a dramatic improvement in the fit performance of the Kalman filter.

There was a three-accelerometer array at the center of the dummy's head in the dummy lateral impact test. The residuals for these observables, which were not included in the fit, were as large as 22 g. Better engineering understanding of the experimental setup should help improve these Kalman filter predictions.

The fore-aft (eyes out) impact tests had a restricted amount of data. Only the two coordinates in the impact plane were recorded for the head photographic fiducials, besides having only three-accelerometer array output. The Kalman filter tracked the observables until

the start of the impact event, at which point it diverged with some residuals being greater than 10^3 g. The cause of this divergence requires further investigation.

The covariance simulation mode of the Kalman filter software was utilized on a lateral impact test to determine the improvement to be obtained with a three-axis angular accelerometer. However, the real advantage of an angular accelerometer is to counteract the effect of piezoresistive accelerometer array dimensional and cross axis biases. Such bias states would have to be added to the present Kalman filter to obtain meaningful results from a covariance simulation.

1.4 FURTHER WORK

The sled impact Kalman filter Fortran IV software should be converted to run on the Wright-Patterson Air Force Base (WPAFB) CDC 6600 computer. The various tests used in debugging the software should be performed, and the fits to data reported herein repeated. If changes are made to individual subroutines at The Charles Stark Draper Laboratory, Inc. (CSDL), they can be incorporated in the CDC 6600 version of the program.

The day-to-day analysis of on-going and past experiments is best done at WPAFB. Refinements to the analysis technique are most expeditiously done at CSDL.

It is sound engineering practice to first apply the Kalman filter tool to accelerometer array data in a more controlled environment than exists in a sled test. Namely, a special fixture is used to impart known linear and angular accelerations to an accelerometer array for scale factor determinations. The data from such calibration tests should be analyzed with the Kalman filter software. States would have to be added for scale factors, cross axis sensitivities, misalignments, etc. Besides checking the model and software in a controlled situation, greater understanding and more accurate scale factors and other coefficients will be determined for the accelerometer array.

A more thorough understanding of the coordinates and orientations in the various experiments should be developed, and the data analyses of this report repeated to see if the fits can be improved. In particular, it should be determined how well photographic fiducial data combined with three-accelerometer mouthpiece array data (rather than nine-accelerometer array data) can describe head motion in an impact experiment.

The software should be made to handle other experimental orientations besides lateral and fore-aft impacts. Nonstationary initial conditions should be tried, such as with a sled traveling down the track and hitting a barrier, e.g., a water brake.

The presentation of experimental results should be improved. For example, there should be software to calculate angular velocities and accelerations at the center of the head and other points beside the center of the accelerometer array using the quaternion formulation.

The motion of other parts of the body should be addressed. There are whole body models of greater or lesser complexity with the various discrete parts attached to each other. A Kalman filter with a greatly expanded number of states could be devised to simultaneously process observables of the various body parts using these body models with the constraint that the body parts are attached to each other. The Kalman filter technique could also be applied to accelerometer and photographic observables of the individual body parts without the complexity and difficulty of considering whole body models.

If the problem of applying the Kalman filter with whole body models is addressed, then other observables could be employed, such as body pressure readings on the seat or belt restraints. If an angular accelerometer is employed, then the angular accelerometer observable formulas and code should be changed to reflect the characteristics of the actual rather than ideal instrument

As the sled impact Kalman filter software matures, more formal documentation should be generated. For the present, the program is to some extent self-documenting with extensive comments in each subroutine.

SECTION 2

QUATERNION REPRESENTATION FOR ROTATIONS

2.1 QUATERNION ALGEBRA

A quaternion, a, is a 4-vector:

$$a = (a_1, a_2, a_3, a_4) \tag{1}$$

where the a_i are real numbers (i = 1, ... 4). Addition and multiplication of quaternions are defined by:

$$a + b = (a_1 + b_1, a_2 + b_2, a_3 + b_3, a_4 + b_4) \tag{2}$$

$$\begin{aligned} a \cdot b = (&a_1b_1 - a_2b_2 - a_3b_3 - a_4b_4, \\ &a_1b_2 + a_2b_1 + a_3b_4 - a_4b_3, \\ &a_1b_3 + a_3b_1 + a_4b_2 - a_2b_4, \\ &a_1b_4 + a_4b_1 + a_2b_3 - a_3b_2) \end{aligned} \tag{3}$$

Note that a·b is not necessarily equal to b·a. The product of a real number α and a quaternion a is:

$$\alpha a = (\alpha a_1, \alpha a_2, \alpha a_3, \alpha a_4) \tag{4}$$

The conjugate a* of a quaternion a is

$$a^* = (a_1, a_2, a_3, a_4)^* = (a_1, -a_2, -a_3, -a_4) \tag{5}$$

so that

$$(ab)^* = b^*a^*, \quad a^{**} = a \tag{6}$$

The absolute value squared of a quaternion a is the positive real number:

$$|a|^2 = aa^* = (a_1^2 + a_2^2 + a_3^2 + a_4^2 , 0, 0, 0,) \tag{7}$$

The multiplicative inverse a^{-1} of a is:

$$a^{-1} = \frac{a^*}{|a|^2} \tag{8}$$

since

$$a \cdot \frac{a^*}{|a|^2} = \frac{a^*}{|a|^2} \cdot a = (1, 0, 0, 0) \tag{9}$$

the quaternion identity. The above properties are summarized by saying that the quaternions are a *noncommutative number field*, a fact originally discovered by Hamilton.

A quaternion number a is a pure real number if $a^* = a$ and a pure quaternion (i.e., real part zero) if $a^* = -a$. For any nonzero quaternion q the transformation

$$a \rightarrow qaq^{-1} \tag{10}$$

is called an inner automorphism of the quaternion number field. It preserves arithmetic operations in the sense that

$$q(a + b)q^{-1} = (qaq^{-1}) + (qbq^{-1}) \tag{11}$$

$$q(ab)q^{-1} = (qaq^{-1})(qbq^{-1}) \tag{12}$$

$$|qaq^{-1}|^2 = |a|^2 \tag{13}$$

If $q' = \alpha q$, where α is a real number, then q' and q define the same inner automorphism. Therefore, we can impose the constraint

$$qq^* = 1 \tag{14}$$

and the inner automorphism can be written as

$$a \rightarrow qaq^* \tag{15}$$

With the constraint Equation (14) there is still a twofold ambiguity in the sense that q and -q define the same inner automorphism.

2.2 ROTATIONS IN 3-SPACE

Let v be a quaternion with zero real part, $v^* = -v$. It can be regarded as a vector in 3-space. If q is any quaternion satisfying constraint Equation (14), then qvq^* also has zero real part. Thus,

$$v \rightarrow qvq^* \tag{16}$$

represents a linear transformation into 3-space. Conversely, any linear transformation (or rotation) of 3-space into 3-space can be represented by a quaternion inner automorphism Equation (16)[1].

It is a two-valued representation, in that both q and -q represent the same linear transformation. The quaternion representation can be thought of as the square root of a linear orthogonal transformation of 3-space.

The quaternion representation for a rotation only requires one constraint Equation (14) on its four components. The nine elements in a 3×3 direction cosine matrix require six constraints to represent a rotation. The three Euler angle parameters represent a rotation with no constraints. However, there is the problem of gimbal lock (a partial derivative matrix singularity for certain values of the angles) and having dynamical equations involving white noise with sines and cosines of Euler angles is less tractible than assuming white noise in the quaternion components.

Given an initial choice for one of the two possible quaternions representing the initial orientation of the instrument frame [say (1, 0, 0, 0)], the choice for time increments after the initial time is defined by continuity.

2.3 CORRESPONDENCE WITH MATRICES

An explicit expression for automorphism Equation (15) is by Equation (3):

$$
\begin{aligned}
qaq^* \quad = \quad & [(q_1^2 + q_2^2 + q_3^2 + q_4^2)a_1, \\
& (q_1^2 + q_2^2 - q_3^2 - q_4^2)a_2 + 2(q_2q_3 - q_1q_4)a_3 \\
& + \ 2(q_1q_3 + q_2q_4)a_4, \\
& 2(q_1q_4 + q_2q_3)a_2 + (q_1^2 - q_2^2 + q_3^2 - q_4^2)a_3 \\
& + \ 2(q_3q_4 - q_1q_2)a_4, \\
& 2(q_2q_4 - q_1q_3)a_2 + 2(q_1q_2 + q_3q_4)a_3 \\
& + \ (q_1^2 - q_2^2 - q_3^2 - q_4^2)a_4]
\end{aligned} \tag{17}
$$

By Equations (7) and (14), a_1 is left fixed. In particular, as proved above, a 3-vector with $a_1 = 0$ is mapped into a 3-vector.

By Equation (17) the transformation matrix corresponding to the vector transformation defined by a quaternion q is

$$
\begin{bmatrix}
(q_1^2 + q_2^2 - q_3^2 - q_4^2) & 2(q_2q_3 - q_1q_4) & 2(q_1q_3 + q_2q_4) \\
2(q_1q_4 + q_2q_3) & (q_1^2 - q_2^2 + q_3^2 - q_4^2) & 2(q_3q_4 - q_1q_2) \\
2(q_2q_4 - q_1q_3) & 2(q_1q_2 + q_3q_4) & (q_1^2 - q_2^2 - q_3^2 + q_4^2)
\end{bmatrix} \tag{18}
$$

As mentioned above, q and -q map into the same linear transformation.

Infinitessimal rotations by angles $\delta\theta_1$, $\delta\theta_2$, $\delta\theta_3$ about the three coordinate axes yield a transformation matrix:

$$
\begin{bmatrix}
1 & \delta\theta_3 & -\delta\theta_2 \\
-\delta\theta_3 & 1 & \delta\theta_1 \\
\delta\theta_2 & -\delta\theta_1 & 1
\end{bmatrix} \tag{19}
$$

Therefore, the quaternion corresponding to this infinitessimal transformation is:

$$q = (1, -\frac{\delta\theta_1}{2}, -\frac{\delta\theta_2}{2}, -\frac{\delta\theta_3}{2}) \tag{20}$$

or -q, where the squares of the small angles in radians are ignored.

Let θ_i be a finite rotation angle about coordinate direction i. The rotation matrix and rotation quaternion for each such finite rotation are:

$$\begin{bmatrix} 1 & 0 & 0 \\ 0 & \cos\theta_1 & \sin\theta_1 \\ 0 & -\sin\theta_1 & \cos\theta_1 \end{bmatrix} \leftrightarrow q = (\cos\frac{\theta_1}{2}, -\sin\frac{\theta_1}{2}, 0, 0) \tag{21}$$

$$\begin{bmatrix} \cos\theta_2 & 0 & \sin\theta_2 \\ 0 & 1 & 0 \\ -\sin\theta_2 & 0 & \cos\theta_2 \end{bmatrix} \leftrightarrow q = (\cos\frac{\theta_2}{2}, 0, -\sin\frac{\theta_2}{2}, 0) \tag{22}$$

$$\begin{bmatrix} \cos\theta_3 & \sin\theta_3 & 0 \\ -\sin\theta_3 & \cos\theta_3 & 0 \\ 0 & 0 & 1 \end{bmatrix} \leftrightarrow q = (\cos\frac{\theta_3}{2}, 0, 0, -\sin\frac{\theta_3}{2}) \tag{23}$$

or -q in each case.

An Euler angle transformation matrix can be expressed as the product of three simple rotation matrices such as above. Namely, let (X, Y, Z) be one coordinate system and (X', Y', Z') another with Euler angles given in Figure 2-1:

Ω = angle between the X axis and the intersection of the (X', Y') plane on the (X, Y) plane measured along the (X, Y) plane ($0 \leq \Omega < 360°$)

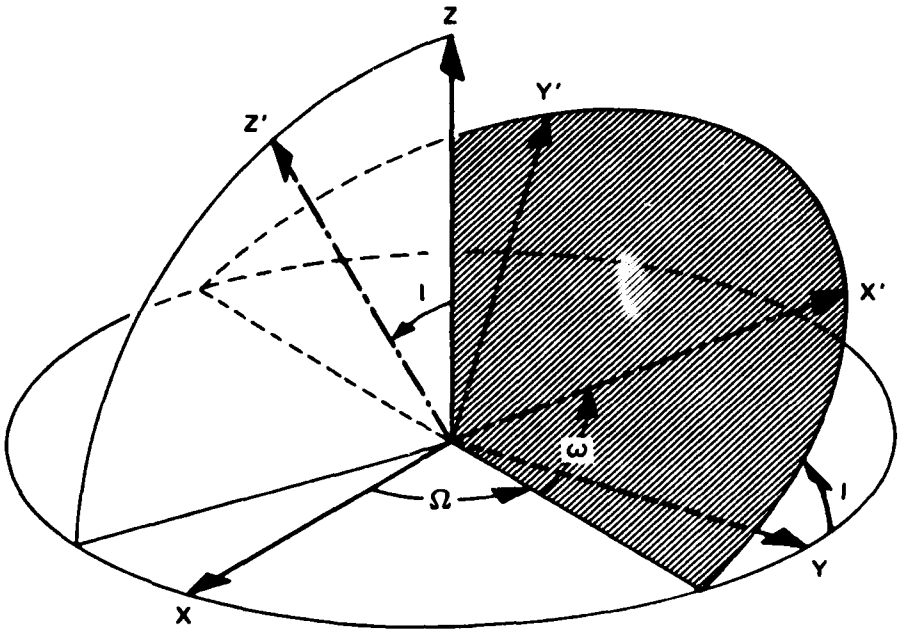

Figure 2-1. Euler angles.

I = angle between the (X, Y) plane and the (X', Y') plane ($0 \leq I \leq 180°$)

ω = angle between the intersection of the (X', Y') on the (X, Y) plane and the X' axis measured along the (X', Y') plane ($0 \leq \omega < 360°$)

The transformation

$$\begin{bmatrix} X' \\ Y' \\ Z' \end{bmatrix} = \begin{bmatrix} A_{11} & A_{12} & A_{13} \\ A_{21} & A_{22} & A_{23} \\ A_{31} & A_{32} & A_{33} \end{bmatrix} \begin{bmatrix} X \\ Y \\ Z \end{bmatrix} \quad (24)$$

is

$$
\begin{aligned}
A_{11} &= \cos\Omega\cos\omega - \sin\Omega\sin\omega\cos I \\
A_{12} &= \sin\Omega\cos\omega + \cos\Omega\sin\omega\cos I \\
A_{13} &= \sin\omega\sin I \\
A_{21} &= -\cos\Omega\sin\omega - \sin\Omega\cos\omega\cos I \\
A_{22} &= -\sin\Omega\sin\omega + \cos\Omega\cos\omega\cos I \\
A_{23} &= \cos\omega\sin I \\
A_{31} &= \sin\Omega\sin I \\
A_{32} &= -\cos\Omega\sin I \\
A_{33} &= \cos I
\end{aligned} \tag{25}
$$

It results from a rotation about Z by an angle Ω, about the new Y axis by an angle I, and about the new-new Z axis (= Z') by an angle ω. Thus, the quaternion corresponding to the Euler angle transformation matrix (25) is

$$
\begin{aligned}
q \approx\ & (\cos\tfrac{\Omega}{2},\ 0,\ 0,\ -\sin\tfrac{\Omega}{2}) \cdot \\
& \cdot(\cos\tfrac{I}{2},\ 0,\ -\sin\tfrac{I}{2},\ 0) \cdot \\
& \cdot(\cos\tfrac{\omega}{2},\ 0,\ 0,\ -\sin\tfrac{\omega}{2}) \\
= (&\cos\tfrac{\Omega}{2}\cos\tfrac{I}{2}\cos\tfrac{\omega}{2} - \sin\tfrac{\Omega}{2}\sin\tfrac{I}{2}\sin\tfrac{\omega}{2}, \\
&\cos\tfrac{\Omega}{2}\sin\tfrac{I}{2}\sin\tfrac{\omega}{2} - \sin\tfrac{\Omega}{2}\sin\tfrac{I}{2}\cos\tfrac{\omega}{2}, \\
&-\cos\tfrac{\Omega}{2}\sin\tfrac{I}{2}\cos\tfrac{\omega}{2} - \sin\tfrac{\Omega}{2}\sin\tfrac{I}{2}\sin\tfrac{\omega}{2}, \\
&-\cos\tfrac{\Omega}{2}\cos\tfrac{I}{2}\sin\tfrac{\omega}{2} - \sin\tfrac{\Omega}{2}\cos\tfrac{I}{2}\cos\tfrac{\omega}{2})
\end{aligned} \tag{26}
$$

Consider a general direction cosine orthogonal matrix:

$$A = \begin{bmatrix} A_{11} & A_{12} & A_{13} \\ A_{21} & A_{22} & A_{23} \\ A_{31} & A_{32} & A_{33} \end{bmatrix} \tag{27}$$

The orthogonality condition is that the inverse is equal to the transpose $A^{-1} = A^T$:

$$\sum_{k=1}^{3} A_{ik} A_{jk} = \delta_{ij} = \begin{cases} 1 \text{ if } i = j \\ 0 \text{ if } i \neq j \end{cases} \tag{28}$$

Equation (18) gives the A corresponding to a quaternion q. Given the constraint Equations (7) and (14), checking that matrix (18) satisfies condition (28) is straightforward.

Suppose a matrix (27) is given satisfying the conditions (28). Presuming that matrix (27) can be expressed in the form (18), it follows that

$$2(q_1^2 - q_4^2) = A_{11} + A_{22} \tag{29a}$$

$$2(q_1^2 - q_2^2) = A_{22} + A_{33} \tag{29b}$$

$$2(q_1^2 - q_3^2) = A_{11} + A_{33} \tag{29c}$$

$$2(q_2^2 - q_3^2) = A_{11} - A_{22} \tag{29d}$$

$$2(q_2^2 - q_4^2) = A_{11} - A_{33} \tag{29e}$$

$$2(q_3^2 - q_4^2) = A_{22} - A_{33} \tag{29f}$$

$$4q_2q_3 = A_{12} + A_{21} \tag{29g}$$

$$4q_2q_4 = A_{13} + A_{31} \tag{29h}$$

$$4q_3q_4 = A_{23} + A_{32} \tag{29i}$$

$$4q_1q_2 = A_{32} - A_{23} \tag{29j}$$

$$4q_1q_3 = A_{13} - A_{31} \tag{29k}$$

$$4q_1q_4 = A_{21} - A_{12} \tag{29l}$$

$$\frac{q_2}{q_3} = \frac{A_{13} + A_{31}}{A_{23} + A_{32}} = \frac{A_{32} - A_{23}}{A_{13} - A_{31}} \qquad (29m)$$

$$\frac{q_2}{q_4} = \frac{A_{12} + A_{21}}{A_{23} + A_{32}} = \frac{A_{32} - A_{23}}{A_{21} - A_{12}} \qquad (29n)$$

$$\frac{q_3}{q_4} = \frac{A_{12} + A_{21}}{A_{13} + A_{31}} = \frac{A_{13} - A_{31}}{A_{21} - A_{12}} \qquad (29o)$$

By Equations (29d, m) and (29 e, n)

$$q_2^2 = \frac{(A_{13} + A_{31})(A_{11} - A_{22})}{2(A_{13} + A_{31} - A_{23} - A_{32})}$$

$$= \frac{(A_{32} - A_{23})(A_{11} - A_{22})}{2(A_{32} - A_{23} - A_{13} + A_{31})}$$

$$= \frac{(A_{12} + A_{21})(A_{22} - A_{33})}{2(A_{12} + A_{21} - A_{23} - A_{32})}$$

$$= \frac{(A_{21} - A_{12})(A_{22} - A_{33})}{2(A_{21} - A_{12} - A_{32} + A_{23})} \qquad (30)$$

By Equations (29d, m) and (29f, o)

$$q_3^2 = \frac{(A_{23} + A_{32})(A_{11} - A_{22})}{2(A_{13} + A_{31} - A_{23} - A_{32})}$$

$$= \frac{(A_{13} - A_{31})(A_{11} - A_{22})}{2(A_{32} - A_{23} - A_{13} + A_{31})}$$

$$= \frac{(A_{12} + A_{21})(A_{22} - A_{33})}{2(A_{12} + A_{21} - A_{13} - A_{31})}$$

$$= \frac{(A_{13} - A_{31})(A_{22} - A_{33})}{2(A_{13} - A_{31} - A_{21} + A_{12})} \qquad (31)$$

By Equations (29e, n) and (29f, o)

$$q_4^2 = \frac{(A_{23} + A_{32})(A_{11} - A_{33})}{2(A_{12} + A_{21} - A_{23} - A_{32})}$$

$$= \frac{(A_{21} - A_{12})(A_{11} - A_{33})}{2(A_{32} - A_{23} - A_{21} + A_{12})}$$

$$= \frac{(A_{13} + A_{31})(A_{22} - A_{33})}{2(A_{12} + A_{21} - A_{13} - A_{31})}$$

$$= \frac{(A_{21} - A_{12})(A_{22} - A_{33})}{2(A_{13} - A_{31} - A_{21} + A_{12})} \qquad (32)$$

The expressions in Equations (30), (31), and (32) with the largest denominators should be chosen to evaluate q_2^2, q_3^2, and q_4^2. The component q_1^2 can then be calculated from any of Equations (29a, b, c). A choice of sign for q_1 determines the signs of q_2, q_3, and q_4 by Equations (29j, k, l). There should be no inconsistencies in deriving the q corresponding to an A if orthogonal conditions (28) hold and if no reflections are involved.

If all the denominators in Equations (30), (31), and (32) were zero, A would have to be a diagonal matrix with ±1 on the diagonal. There can be none or two -1s, since otherwise a reflection is involved and quaternions do not map into reflections, only rotations. The quaternions corresponding to the allowed diagonal rotation matrices are given in Equations (21), (22), and (23) with $\theta_i = 0°, 180°$.

For completeness, the Euler angles corresponding to a rotation matrix A are given:

$$\left.\begin{aligned} \sin I &= \sqrt{A_{31}^2 + A_{32}^2} \\ \cos I &= A_{11}A_{22} - A_{12}A_{21} \end{aligned}\right\} \quad 0° \leq I \leq 180° \qquad (33)$$

$$\left.\begin{aligned} \sin \omega &= A_{31}/\sin I \\ \cos \omega &= A_{32}/\sin I \end{aligned}\right\} \quad 0° \leq \omega < 360° \qquad (34)$$

$$\left.\begin{aligned} \sin \Omega &= A_{21}\cos \omega - A_{22}\sin \omega \\ \cos \Omega &= A_{11}\cos \omega - A_{12}\sin \omega \end{aligned}\right\} \quad 0° \leq \Omega < 360° \qquad (35)$$

2.4 ANGULAR VELOCITY

Let $\vec{r} = (r_1, r_2, r_3)^T$ be body fixed column vector with the transformation to another coordinate system being defined by

$$\vec{s} = A\vec{r} \qquad (36)$$

where A is a rotation matrix which is a function of time. Then

$$A^T \frac{d\vec{s}}{dt} = A^T \frac{dA}{dt} \vec{r}$$

$$= \begin{bmatrix} 0 & -\omega_3 & \omega_2 \\ \omega_3 & 0 & -\omega_1 \\ -\omega_2 & \omega_1 & 0 \end{bmatrix} \vec{r}$$

$$= \vec{\omega} \times \vec{r} \qquad (37)$$

because of the orthogonality condition Equation (28).

Consider the corresponding quaternion expressions with $r = (0, r_1, r_2, r_3)$:

$$s = qrq^* \tag{38}$$

$$q^*\frac{ds}{dt}q = q^*\frac{dq}{dt}r + r\frac{dq^*}{dt}q \tag{39}$$

Constraint Equation (14) implies

$$\frac{dq}{dt}q^* + q\frac{dq^*}{dt} = 0 \tag{40}$$

$$\frac{d^2q}{dt^2}q^* + 2\frac{dq}{dt}\frac{dq^*}{dt} + q\frac{d^2q^*}{dt^2} = 0 \tag{41}$$

Let

$$\bar{\omega} = (0, \bar{\omega}_1 \ \bar{\omega}_2 \ \bar{\omega}_3) = 2q^*\frac{dq}{dt} \tag{42}$$

The real part of ω is zero by Equation (40). Then Equation (39) can be written

$$q^*sq = \frac{1}{2}\left[\bar{\omega}r - r\bar{\omega}\right] \tag{43}$$

which is the Poisson bracket. Carring out the indicated operations yields

$$\frac{1}{2}\left[\bar{\omega}r - r\bar{\omega}\right] = (0, \ \bar{\omega}_2r_3 - \bar{\omega}_3r_2, \ \bar{\omega}_3r_1 - \bar{\omega}_1r_3, \ \bar{\omega}_2r_3 - \bar{\omega}_3r_2) \tag{44}$$

which is the quaternion equivalent to $\vec{\omega} \times \vec{r}$. Thus

$$\bar{\omega}_1 = \omega_1, \ \bar{\omega}_2 = \omega_2, \ \bar{\omega}_3 = \omega_3 \tag{45}$$

and the quaternion Poisson bracket corresponds to vector cross product.

2.5 ANGULAR ACCELERATION

Differentiation of Equation (37) gives the matrix form for angular acceleration in the body fixed frame

$$A^T \frac{d^2\vec{s}}{dt^2} = \frac{d\vec{\omega}}{dt} \times \vec{r} + \vec{\omega} \times \vec{\omega} \times \vec{r} \tag{46}$$

assuming that the vector $\vec{r}$ is fixed in the body. Differentiation of Equation (43) gives the quaternion equivalent

$$q^* \frac{d^2 s}{dt^2} q = \frac{1}{2}\left[\frac{d\bar{\omega}}{dt} r - r \frac{d\bar{\omega}}{dt}\right] + \frac{1}{4}\left[\bar{\omega}\left[\bar{\omega} r - r\bar{\omega}\right] - \left[\bar{\omega} r - r\bar{\omega}\right]\bar{\omega}\right] \tag{47}$$

SECTION 3
DYNAMICAL SYSTEM EQUATIONS

3.1 COORDINATE SYSTEMS

In Figure 3-1, a human or dummy subject is seated on a sled which is constrained to move down a track for a lateral impact test. Figure 3-2 is a similar representation of a fore-aft (eyes out) impact test.

There is a 9-accelerometer array on the side of subject's head in Figure 3-1, and a 3-accelerometer array inside the subject's mouth in Figure 3-2. Let the coordinate system (X, Y, Z) be fixed in the linear accelerometer array with origin at the center of the accelerometer array such that

X = positive forward out of the subject's head

Z = positive towards the top of the subject's head

Y = completes the right hand system (positive towards the subject's left side)

Define a coordinate system ($\bar{X}$, $\bar{Y}$, $\bar{Z}$) fixed in the sled seat by

$\bar{X}$ = forward out of the seat

$\bar{Z}$ = positive up

$\bar{Y}$ = completes the right hand system

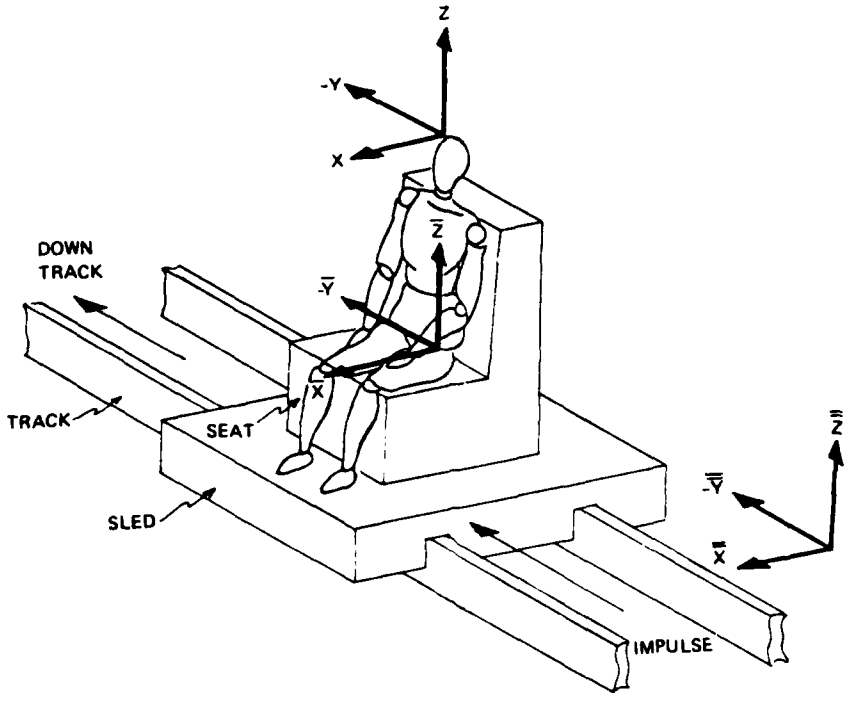

Figure 3-1. Lateral impact sled test coordinates.

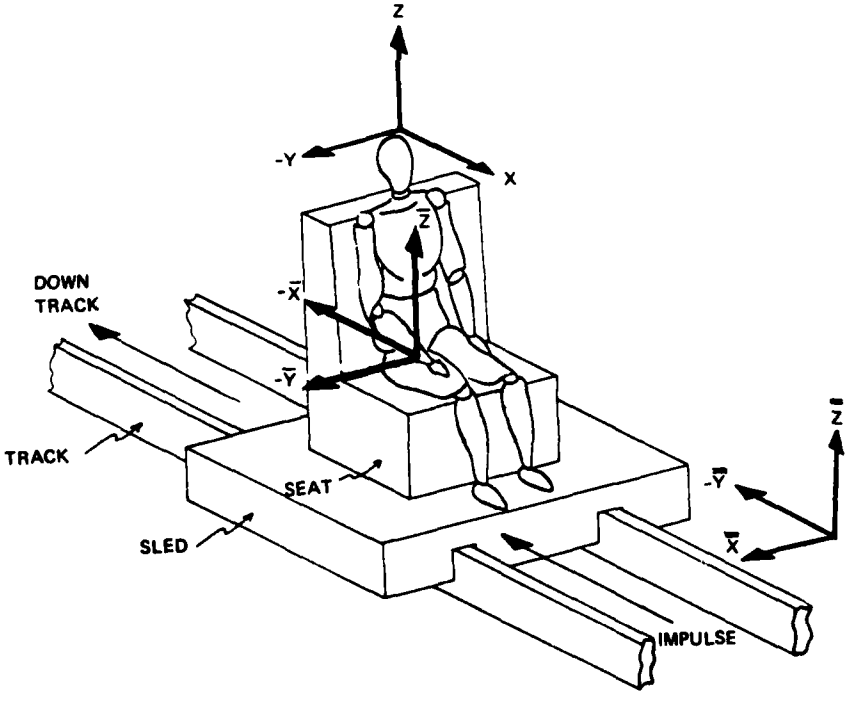

Figure 3-2. Fore-aft (eyes out) impact sled test coordinates.

Initially, the $(\bar{X}, \bar{Y}, \bar{Z})$ axes are parallel to the (X, Y, Z) axes for an upright subject. The origin of the sled coordinates could vary between experiments.

Finally, the laboratory coordinate system $(\bar{\bar{X}}, \bar{\bar{Y}}, \bar{\bar{Z}})$ fixed in the track is

$-\bar{\bar{Y}}$ = along the track in the direction of motion

$\bar{\bar{Z}}$ = positive up

$\bar{\bar{X}}$ = completes the right hand system

For a lateral impact test, the $(\bar{\bar{X}}, \bar{\bar{Y}}, \bar{\bar{Z}})$ axes are parallel to the $(\bar{X}, \bar{Y}, \bar{Z})$ axes. For a fore-aft (eyes out) impact test, $-\bar{\bar{Y}}$ is parallel to $-\bar{X}$ and $\bar{\bar{X}}$ is parallel to $-\bar{Y}$. The origins of the $(\bar{X}, \bar{Y}, \bar{Z})$ and $(\bar{\bar{X}}, \bar{\bar{Y}}, \bar{\bar{Z}})$ coordinate systems are assumed to coincide at time t_0.

At time t, let

$$\left.\begin{aligned} \bar{X} &= \bar{\bar{X}} \\ \bar{Y} &= \bar{\bar{Y}} + y_1(t) \\ \bar{Z} &= \bar{\bar{Z}} \end{aligned}\right\} \quad \text{lateral impact test} \qquad (48a)$$

$$\left.\begin{aligned} \bar{X} &= \bar{\bar{Y}} + y_1(t) \\ \bar{Y} &= -\bar{\bar{X}} \\ \bar{Z} &= \bar{\bar{Z}} \end{aligned}\right\} \quad \text{fore-aft (eyes out) impact test} \qquad (48b)$$

where

$$y_1(t_0) = 0$$
$$y_1(t) > 0, \quad t > t_0 \qquad (49)$$

with t_0 being the time of initiation of the experiment when the impact is imparted to the sled in Figures 3-1 or 3-2.

Let the transformation from accelerometer array coordinates (X, Y, Z) to sled coordinates $(\bar{X}, \bar{Y}, \bar{Z})$ be

$$(0, \bar{X}, \bar{Y}, \bar{Z}) = (0, z_1(t), z_2(t), z_3(t)) + q(t)(0, X, Y, Z)q(t)^* \quad (50)$$

where the quaternion $q = (q_1, q_2, q_3, q_4)$ defines a rotation and $z = (0, z_1, z_2, z_3)$ defines a translation. The initial conditions might be

$$z(t_0) = (0, z_{10}, z_{20}, z_{30}) \quad (51)$$

$$q(t_0) = (1, 0, 0, 0) \quad (52)$$

for an upright initially stationary subject.

3.2 EQUATIONS OF STATE

The state variables which give the dynamical system representation of the impact experiment are

y_1 = position of the sled frame relative to the track frame (cm)

y_2 = velocity of the sled frame relative to the track frame (cm/s)

y_3 = acceleration of the sled frame relative to the track frame (cm/s^2)

z_1, z_2, z_3 = translational position of the center of the accelerometer array frame relative to the sled frame (cm)

z_4, z_5, z_6 = translational velocity of the center of the accelerometer array frame relative to the sled frame (cm/s)

z_7, z_8, z_9 = translational acceleration of the center of the accelerometer array frame relative to the sled frame (cm/s^2)

q_1, q_2, q_3, q_4 = quaternion rotational position of the accelerometer array frame relative to the sled frame (dimensionless)

q_5, q_6, q_7, q_8 = quaternion rotational velocity of the accelerometer array frame relative to the sled frame (s^{-1})

$q_9, q_{10}, q_{11}, q_{12}$ = quaternion rotational acceleration of the accelerometer array frame relative to the sled frame (s^{-2})

The dynamical equations satisfied by these 24 state variables are

$$\frac{dy_1}{dt} = y_2 + w_1$$

$$\frac{dy_2}{dt} = y_3 + w_2$$

$$\frac{dy_3}{dt} = 0 + w_3$$

$$\frac{dz_j}{dt} = z_{j+3} + w_{3+j}, \quad j = 1, \ldots, 6$$

$$\frac{dz_j}{dt} = 0 + w_{3+j}, \quad j = 7, 8, 9$$

$$\frac{dq_j}{dt} = q_{j+4} + w_{12+j}, \quad j = 1, \ldots, 8$$

$$\frac{dq_j}{dt} = 0 + w_{12+j}, \quad j = 9, \ldots, 12 \qquad (53)$$

where $\vec{w} = (w_1, \ldots, w_{24})$ is zero mean Gausian white noise in the dynamics. The constraint Equations (7) and (14) imply

$$\sum_{i=1}^{4} q_i^2 = 1 \tag{54}$$

$$\sum_{i=1}^{4} q_i q_{i+4} = 0 \tag{55}$$

$$\sum_{i=1}^{4} q_i q_{i+8} = -\sum_{i=1}^{4} q_{i+4}^2 \tag{56}$$

The dynamics in Equation (53) are simplistic. Still, they allow observations at different times to be tied together, and will propagate an impact trajectory which best fits diverse observation types (e.g., accelerometer and photographic) using Kahman filter and smoother state estimation formulas. The covariance of the integral of the noise process (w_1, ... , w_{24}) in the Kalman gain matrix has to be judiciously chosen to match the impact profile of the specific experiment (see Section 7.4).

The dynamics of the z and q states defining the transformation Equation (50) between the sled and accelerometer array frames is constrained by the human body dynamics. A finite element model of the human body with more states than used above could have more realistic dynamic equations than the simplistic model employed in Equations (53).

3.3 INTEGRATION OF THE STATE EQUATIONS

Let ($y_1(t_k)$, ... , $q_{12}(t_k)$) be the estimates of the state variables at time t_k. For time t_0, these are just the initial condition of the experiment, which could be Equations (49), (51), and (52) plus zero velocities and accelerations for an initially stationary subject. For time t_k they represent the propagation of the state by the dynamical equations with updates from the observations between times t_1 and t_k. It is presumed that the quaternion states

$$(q_1(t_k), \ldots , q_{12}(t_k))$$

satisfy the constraint Equations (54), (55), and (56).

The state at time t_{k+1} given the state at time t_k and assuming zero mean noise is by Equations (53)

$$
\begin{aligned}
y_1(t_{k+1}|t_k) &= y_1(t_k) + y_2(t_k)(t_{k+1} - t_k) \\
&\quad + \frac{1}{2} y_3(t_k)(t_{k+1} - t_k)^2 \\
y_2(t_{k+1}|t_k) &= y_2(t_k) + y_3(t_k)(t_{k+1} - t_k) \\
y_3(t_{k+1}|t_k) &= y_3(t_k) \\
z_j(t_{k+1}|t_k) &= z_j(t_k) + z_{j+3}(t_k)(t_{k+1} - t_k) \\
&\quad + \frac{1}{2} z_{j+6}(t_k)(t_{k+1} - t_k)^2, \\
&\quad j = 1, 2, 3 \\
z_{j+3}(t_{k+1}|t_k) &= z_{j+3}(t_k) + z_{j+6}(t_k)(t_{k+1} - t_k), \\
&\quad j = 1, 2, 3 \\
z_{j+6}(t_{k+1}|t_k) &= z_{j+6}(t_{k+1}), \\
&\quad j = 1, 2, 3 \\
\bar{q}_j(t_{k+1}|t_k) &= q_j(t_k) + q_{j+4}(t_k)(t_{k+1} - t_k) \\
&\quad + \frac{1}{2} q_{j+8}(t_k)(t_{k+1} - t_k)^2, \\
&\quad j = 1, \ldots, 4 \\
\bar{q}_{j+4}(t_{k+1}|t_k) &= q_{j+4}(t_k) + q_{j+8}(t_k)(t_{k+1} - t_k) \\
&\quad j = 1, \ldots, 4 \\
\bar{q}_{j+8}(t_{k+1}|t_k) &= q_{j+8}(t_k), \\
&\quad j = 1, \ldots, 4
\end{aligned}
\tag{57}
$$

where bars are put over the q variables because they are intermediate to the final variables which satisfy the constraints Equations (54), (55), and (56).

3.4 QUATERNION CONSTRAINTS

The $(\bar{q}_1, \ldots, \bar{q}_{12})$ satisfy the constraints except for higher order terms in $(t_{k+1} - t_k)$. In order to satisfy the constraints exactly, let

$$q_j(t_{k+1}|t_k) = \frac{\bar{q}_j(t_{k+1}|t_k)}{\left[\sum_{i=1}^{4} \bar{q}_i(t_{k+1}|t_k)^2\right]^{1/2}},$$

$$j = 1, \ldots, 4 \tag{58}$$

$$q_{j+4}(t_{k+1}|t_k) = \bar{q}_{j+4}(t_{k+1}|t_k) - \left[\sum_{i=1}^{4} q_i(t_{k+1}|t_k)\bar{q}_{i+4}(t_{k+1}|t_k)\right] \cdot q_j(t_{k+1}|t_k),$$

$$j = 1, \ldots, 4 \tag{59}$$

$$q_{j+8}(t_{k+1}|t_k) = \bar{q}_{j+8}(t_{k+1}|t_k) - \left[\sum_{i=1}^{4} q_i(t_{k+1}|t_k)\bar{q}_{i+8}(t_{k+1}|t_k) + \sum_{i=1}^{4} q_{i+4}(t_{k+1}|t_k)^2\right] \cdot q_j(t_{k+1}|t_k),$$

$$j = 1, \ldots, 4 \tag{60}$$

Taylor series formulas can be used to propagate the differential equations solutions rather than more sophisticated integration techniques because the spacing between observation times t_k and t_{k+1} is of the order of a millisecond, besides the fact that the simplistic dynamical model employed has exact Taylor series solutions.

SECTION 4

STATE TRANSITION MATRIX

4.1 LINEAR MODEL

The state dynamical Equations (53) can be written in the form

$$\frac{d}{dt}\begin{bmatrix} x_1 \\ \cdot \\ \cdot \\ \cdot \\ \cdot \\ x_{24} \end{bmatrix} = A \begin{bmatrix} x_1 \\ \cdot \\ \cdot \\ \cdot \\ \cdot \\ x_{24} \end{bmatrix} + \begin{bmatrix} w_1 \\ \cdot \\ \cdot \\ \cdot \\ \cdot \\ w_{24} \end{bmatrix} \tag{61}$$

where

$$\begin{bmatrix} x_1 \\ \cdot \\ \cdot \\ \cdot \\ \cdot \\ x_{24} \end{bmatrix} = \begin{bmatrix} y_1 \\ y_2 \\ y_3 \\ z_1 \\ \cdot \\ \cdot \\ \cdot \\ \cdot \\ z_9 \\ q_1 \\ \cdot \\ \cdot \\ \cdot \\ \cdot \\ \cdot \\ q_{12} \end{bmatrix} \tag{62}$$

and where the 24 x 24 matrix A is

$$A = \begin{bmatrix} A_{3 \times 3} & & 0 \\ & A_{9 \times 9} & \\ 0 & & A_{12 \times 12} \end{bmatrix} \tag{63}$$

The submatrices of the given dimensions are

$$A_{3 \times 3} = \begin{bmatrix} 0 & 1 & 0 \\ 0 & 0 & 1 \\ 0 & 0 & 0 \end{bmatrix} \tag{64}$$

$$A_{9 \times 9} = \begin{bmatrix} 0 & 0 & 0 & 1 & 0 & 0 & 0 & 0 & 0 \\ 0 & 0 & 0 & 0 & 1 & 0 & 0 & 0 & 0 \\ 0 & 0 & 0 & 0 & 0 & 1 & 0 & 0 & 0 \\ 0 & 0 & 0 & 0 & 0 & 0 & 1 & 0 & 0 \\ 0 & 0 & 0 & 0 & 0 & 0 & 0 & 1 & 0 \\ 0 & 0 & 0 & 0 & 0 & 0 & 0 & 0 & 1 \\ 0 & 0 & 0 & 0 & 0 & 0 & 0 & 0 & 0 \\ 0 & 0 & 0 & 0 & 0 & 0 & 0 & 0 & 0 \\ 0 & 0 & 0 & 0 & 0 & 0 & 0 & 0 & 0 \end{bmatrix} \tag{65}$$

$$A_{12 \times 12} = \begin{bmatrix} 0 & 0 & 0 & 0 & 1 & 0 & 0 & 0 & 0 & 0 & 0 & 0 \\ 0 & 0 & 0 & 0 & 0 & 1 & 0 & 0 & 0 & 0 & 0 & 0 \\ 0 & 0 & 0 & 0 & 0 & 0 & 1 & 0 & 0 & 0 & 0 & 0 \\ 0 & 0 & 0 & 0 & 0 & 0 & 0 & 1 & 0 & 0 & 0 & 0 \\ 0 & 0 & 0 & 0 & 0 & 0 & 0 & 0 & 1 & 0 & 0 & 0 \\ 0 & 0 & 0 & 0 & 0 & 0 & 0 & 0 & 0 & 1 & 0 & 0 \\ 0 & 0 & 0 & 0 & 0 & 0 & 0 & 0 & 0 & 0 & 1 & 0 \\ 0 & 0 & 0 & 0 & 0 & 0 & 0 & 0 & 0 & 0 & 0 & 1 \\ 0 & 0 & 0 & 0 & 0 & 0 & 0 & 0 & 0 & 0 & 0 & 0 \\ 0 & 0 & 0 & 0 & 0 & 0 & 0 & 0 & 0 & 0 & 0 & 0 \\ 0 & 0 & 0 & 0 & 0 & 0 & 0 & 0 & 0 & 0 & 0 & 0 \\ 0 & 0 & 0 & 0 & 0 & 0 & 0 & 0 & 0 & 0 & 0 & 0 \end{bmatrix} \tag{66}$$

The integration of Equation (61) between times t_k and t_{k+1} with white noise $\vec{w}$ set to zero yields

$$\vec{x}(t_{k+1}|t_k) = \Phi(t_{k+1}, t_k)\, \vec{x}(t_k) \tag{67}$$

where the state transition matrix Φ is

$$\Phi(t_{k+1}, t_k) = \exp\,[A(t_{k+1} - t_k)]$$

$$= \sum_{i=0}^{\infty} \frac{1}{i!}[A(t_{k+1} - t_k)]^i \tag{68}$$

By Equation (63) this can be written as

$$\Phi(t_{k+1}, t_k) = \begin{bmatrix} \exp[A_{3X3}(t_{k+1} - t_k)] & & 0 \\ & \exp[A_{9X9}(t_{k+1} - t_k)] & \\ 0 & & \exp[A_{12X12}(t_{k+1} - t_k)] \end{bmatrix} \tag{69}$$

where the matrix exponentials would be evaluated by an appropriate computer subroutine.

Equation (67) is the same solution $\vec{x}(t_{k+1}|t_k)$ as the Taylor series expansions Equations (57), since in the dynamics the jerk (derivative of acceleration) is assumed to be zero. The state transition matrix Φ is the partial derivative of the state at time t_{k+1} with respect to the state at time t_k:

$$\Phi = \frac{\partial \vec{x}(t_{k+1}|t_{k+1})}{\partial \vec{x}(t_k)} \tag{70}$$

Thus, functional relationships Equations (57) allow us to write

$$\frac{\partial y_1(t_{k+1}|t_k)}{\partial y_i(t_k)} = \begin{cases} 1 & i = 1 \\ (t_{k+1} - t_k) & i = 2 \\ \frac{1}{2}(t_{k+1} - t_k)^2 & i = 3 \end{cases} \tag{71}$$

$$\frac{\partial y_2(t_{k+1}|t_k)}{\partial y_i(t_k)} = \begin{cases} 0 & i = 1 \\ 1 & i = 2 \\ (t_{k+1} - t_k) & i = 3 \end{cases} \tag{72}$$

$$\frac{\partial y_3(t_{k+1}|t_k)}{\partial y_i(t_k)} = \begin{cases} 0 & i = 1 \\ 0 & i = 2 \\ 1 & i = 3 \end{cases} \tag{73}$$

$$\frac{\partial z_j(t_{k+1}|t_k)}{\partial z_i(t_k)} = \begin{cases} 1 & i = j \\ (t_{k+1} - t_k) & i = j+3 \\ \frac{1}{2}(t_{k+1} - t_k)^2 & i = j+6 \end{cases} \qquad j = 1, 2, 3 \tag{74}$$

$$\frac{\partial z_{j+3}(t_{k+1}|t_k)}{\partial z_i(t_k)} = \begin{cases} 0 & i = j \\ 1 & i = j+3 \\ (t_{k+1} - t_k) & i = j+6 \end{cases} \qquad j = 1,2,3 \tag{75}$$

$$\frac{\partial z_{j+6}(t_{k+1}|t_k)}{\partial z_i(t_k)} = \begin{cases} 0 & i = j \\ 0 & i = j+3 \\ 1 & i = j+6 \end{cases} \qquad j = 1,2,3 \tag{76}$$

$$\frac{\partial \bar{q}_j(t_{k+1}|t_k)}{\partial q_i(t_k)} = \begin{cases} 1 & i = j \\ (t_{k+1} - t_k) & i = j+4 \\ \frac{1}{2}(t_{k+1} - t_k)^2 & i = j+8 \end{cases} \qquad j = 1,2,3,4 \tag{77}$$

$$\frac{\partial \bar{q}_{j+4}(t_{k+1}|t_k)}{\partial q_i(t_k)} = \begin{cases} 0 & i = j \\ 1 & i = j+4 \\ (t_{k+1} - t_k) & i = j+8 \end{cases} \qquad j = 1,2,3,4 \tag{78}$$

$$\frac{\partial \bar{q}_{j+8}(t_{k+1}|t_k)}{\partial q_i(t_k)} = \begin{cases} 0 & i = j \\ 0 & i = j+4 \\ 1 & i = j+8 \end{cases} \tag{79}$$

with partial derivatives not included in Equation (71) through (79) being zero.

If more complicated linear dynamics are added to Equations (61) than those given by Equations (63) through (66), then the matrix exponential can be used. For now, closed form Equations (71) through (79) can be employed.

4.2 QUATERNION CONSTRAINTS

Normalizing the results as at the end of Section 3 makes the state transition nonlinear, which requires the use of extended Kalman filtering and smoothing. This requirement also arises from nonlinear formulas for the observables in terms of the states.

For the final normalized variables

$$\frac{\partial q_j(t_{k+1}|t_k)}{\partial q_\ell(t_k)} = \sum_{i=1}^{n} \frac{\partial q_j(t_{k+1}|t_k)}{\partial \bar{q}_i(t_{k+1}|t_k)} \frac{\partial \bar{q}_i(t_{k+1}|t_k)}{\partial q_\ell(t_k)}$$

$$j, \ell = 1, \ldots, 12 \tag{80}$$

Let δ_{ij} be the Kronecher delta

$$\delta_{ij} = \begin{cases} 0 & i \neq j \\ 1 & i = j \end{cases} \tag{81}$$

and let

$$\rho = \left[\sum_{i=1}^{4} \bar{q}_i^2 \right]^{1/2} \tag{82}$$

Then constraint Equations (58), (59), and (60) imply for $j = 1, \ldots, 4$

$$\frac{\partial q_j}{\partial \bar{q}_i} = \frac{1}{\rho} \left[\delta_{ij} - \frac{\bar{q}_i \bar{q}_j}{\rho^2} \right] \quad i = 1, \ldots, 4 \tag{83}$$

$$\frac{\partial q_j}{\partial \bar{q}_i} = 0, \quad i = 5, \ldots, 12 \tag{84}$$

$$\frac{\partial q_{j+4}}{\partial \bar{q}_i} = -\left[\sum_{\ell=1}^{4} \frac{\partial q_\ell}{\partial \bar{q}_i}\bar{q}_{\ell+4}\right] q_j - \left[\sum_{\ell=1}^{4} q_\ell \bar{q}_{\ell+4}\right]\frac{\partial q_j}{\partial \bar{q}_i} \qquad i = 1, \ldots, 4 \qquad (85)$$

$$\frac{\partial q_{j+4}}{\partial \bar{q}_i} = \delta_{i-4,j} - q_{i-4}q_j, \qquad i = 5, \ldots, 8 \qquad (86)$$

$$\frac{\partial q_{j+4}}{\partial \bar{q}_i} = 0 \qquad i = 9, \ldots, 12 \qquad (87)$$

$$\frac{\partial q_{j+8}}{\partial \bar{q}_i} = -\left[\sum_{\ell=1}^{4} \frac{\partial q_\ell}{\partial \bar{q}_i}\bar{q}_{\ell+8} + 2\sum_{\ell=1}^{4} q_{\ell+4}\frac{\partial q_{\ell+4}}{\partial \bar{q}_i}\right] q_j - \left[\sum_{\ell=1}^{4} q_\ell \bar{q}_{\ell+8} + \sum_{\ell=1}^{4} q_{\ell+4}^2\right]\frac{\partial q_j}{\partial \bar{q}_i},$$

$$i = 1, \ldots, 4 \qquad (88)$$

$$\frac{\partial q_{j+8}}{\partial \bar{q}_i} = -\left[2\sum_{\ell=1}^{4} q_{\ell+4}\frac{\partial q_{\ell+4}}{\partial \bar{q}_i}\right] q_j, \qquad (89)$$

$$i = 5, \ldots, 8$$

$$\frac{\partial q_{j+8}}{\partial \bar{q}_i} = \delta_{i-8,j} - q_{i-8}q_j, \qquad i = 9, \ldots, 12 \qquad (90)$$

The only problem is that the map from unnormalized to normalized quaternion variables is not one-to-one, which is what is desirable for calculating the state transition Jacobian partial derivative matrix.

For example, let

$$q = \bar{q} = (1, 0, 0, 0)$$

Then

$$\partial q_j / \partial \bar{q}_i = 0 \quad (i, j = 1, \ldots, 4)$$

which cannot be allowed in Equation (80). Since the normalization correction will be very small and the Jacobian partial derivative matrix is only used in propagating the covariance matrix, it will be assumed that

$$\frac{\partial q}{\partial \bar{q}} = 12 \text{ X } 12 \text{ identity matrix} \tag{91}$$

SECTION 5
OBSERVABLES

The theoretical formulas for accelerometer array, ideal angular accelerometer, photographic, track sensor, and quaternion constraint observables are derived in terms of the states

$$y_1, y_2, y_3, z_1, \ldots, z_9, q_1, \ldots, q_{12}$$

5.1 LINEAR ACCELEROMETER ARRAY

Let

b_{i1}, b_{i2}, b_{i3} = position coordinates of linear piezoresistive accelerometer i relative to the center of the accelerometer array in the accelerometer array frame (X, Y, Z)

$\bar{\bar{b}}_{i1}, \bar{\bar{b}}_{i2}, \bar{\bar{b}}_{i3}$ = position coordinates of accelerometer i relative to the laboratory frame $(\bar{\bar{X}}, \bar{\bar{Y}}, \bar{\bar{Z}})$ fixed in the track

c_{i1}, c_{i2}, c_{i3} = direction cosines of the input axis direction of accelerometer i relative to the accelerometer array frame (X, Y, Z)

$\bar{\bar{c}}_{i1}, \bar{\bar{c}}_{i2}, \bar{\bar{c}}_{i3}$ = these direction cosines in the laboratory frame $(\bar{\bar{X}}, \bar{\bar{Y}}, \bar{\bar{Z}})$ fixed in the track

In quaternion notation

$$\begin{aligned} b_i &= (0, b_{i1}, b_{i2}, b_{i3}) \\ \bar{\bar{b}}_i &= (0, \bar{\bar{b}}_{i1}, \bar{\bar{b}}_{i2}, \bar{\bar{b}}_{i3}) \end{aligned} \tag{92}$$

By Equations (48) and (50) the quaternion transformation between the accelerometer array and laboratory frames is

$$\bar{\bar{b}}_i = p[(0, z_1(t), z_2(t), z_3(t)) + q(t)b_i q(t)^*]p^* + (0, 0, -y_1(t), 0) \quad (93)$$

where by Equation (23) with $\theta_3 = 0°, 90°$

$$p = (1, 0, 0, 0) \quad \text{lateral impact test} \quad (94a)$$

$$p = \left(\frac{\sqrt{2}}{2}, 0, 0, -\frac{\sqrt{2}}{2}\right) \quad \text{fore-aft (eyes out) impact test} \quad (94b)$$

The acceleration of accelerometer i relative to the laboratory frame in the laboratory frame is

$$\frac{d^2\bar{\bar{b}}_i}{dt^2} = p\left\{(0, z_7(t), z_8(t), z_9(t)) + \frac{d}{dt^2}[q(t)b_i q(t)^*]\right\} p^* + (0, 0, -y_3(t), 0) \quad (95)$$

where

$$\frac{d^2}{dt^2}[q(t)b_i q(t)^*] = \frac{d^2q(t)}{dt^2} b_i q(t)^* + 2\frac{dq(t)}{dt} b_i \frac{dq(t)^*}{dt} + q(t)b_i \frac{d^2q(t)^*}{dt^2} \quad (96)$$

with

$$\frac{dq(t)}{dt} = \left(\frac{dq_1(t)}{dt}, \frac{dq_2(t)}{dt}, \frac{dq_3(t)}{dt}, \frac{dq_4(t)}{dt}\right) \quad (97)$$

$$= (q_5(t), q_6(t), q_7(t), q_8(t))$$

$$\frac{d^2q(t)}{dt^2} = (q_9(t), q_{10}(t), q_{11}(t), q_{12}(t)) \quad (98)$$

The acceleration sensed by linear accelerometer i is the vector dot product of its input axis direction and the specific acceleration with both being referred to the same reference frame, and where specific acceleration is total acceleration minus the acceleration due to gravity. Either the laboratory frame or the accelerometer array frame could be used. The latter is preferable, since formulas are simplified for cross axis error models and angular accelerometers.

A stationary object in the laboratory frame ($\bar{\bar{X}}$, $\bar{\bar{Y}}$, $\bar{\bar{Z}}$) has a specific acceleration of

$$g = 980.3 \text{ cm/s}^2 \tag{99}$$

along the $\bar{\bar{Z}}$ axis in the vertical up direction, where g is the combination of the accleration due to gravity and the centrifugal acceleration due to the earth's rotation. Thus, the theoretical value of the specific acceleration of accelerometer i referred to the accelerometer array frame is by Equations (95) and (96)

$$\begin{aligned}
\eta_i &= (0, \eta_{i1}, \eta_{i2}, \eta_{i3}) \\
&= q^*p^*\left[\frac{d^2\bar{\bar{b}}_i}{dt^2} + (0, 0, 0, g)\right] pg \\
&= q^*[(0, z_7, z_8, z_9) + p^*(0, 0, -y_3, g)p]q \\
&\quad + \left[\left(q^*\frac{d^2q}{dt^2}\right) b_i + b_i\left(\frac{d^2q^*}{dt^2}q\right)\right. \\
&\quad \left. + 2\left(q^*\frac{dq}{dt}\right) b_i \left(\frac{dq^*}{dt}q\right)\right]
\end{aligned} \tag{100}$$

where it was chosen to keep the result in terms of the quaternion state variables instead of the angular velocity. The theoretical value α_i of accelerometer i output is then

$$\alpha_i = \lambda_a \sum_{j=1}^{3} \eta_{ij} c_{ij} + \mu_i \tag{101}$$

where λ_a is a scale factor to change the internal units of the Kalman Filter-Smoother computer program (cm/s^2) to the accelerometer observable units and where μ_i is a measurement bias.

A piezoresistive accelerometer's output is actually a voltage which is input to an analog-to-digital converter. It is presumed that a scale factor calibration has been performed, and that the observed value of observable α_i has been converted to g. Then the parameter λ_a in Equation (101) is

$$\lambda_a = 1/980.3 \tag{102}$$

For an initially at rest experiment, the bias μ_i is

$$\mu_i = \mu_{i0} - \bar{\bar{c}}_{i3} g \tag{103}$$

where μ_{i0} is the average value of the stationary accelerometer output and where

$$(0, \bar{\bar{c}}_{i1}, \bar{\bar{c}}_{i2}, \bar{\bar{c}}_{i3}) = pq(t_0)(0, c_{i1}, c_{i2}, c_{i3})q(t_0)^*p^* \tag{104}$$

5.2 IDEAL ANGULAR ACCELEROMETER

By Equation (93), the rotation quaternion from the (X, Y, Z) reference frame in which an angular accelerometer is fixed to the $(\bar{\bar{X}}, \bar{\bar{Y}}, \bar{\bar{Z}})$ laboratory reference frame is pq(t). By Equation (42) the angular velocity quaternion ω with components in the (X, Y, Z) reference frame is

$$\begin{aligned} \omega &= (0, \omega_1, \omega_2, \omega_3) \\ &= 2q(t)^* \frac{dq(t)}{dt} \end{aligned} \tag{105}$$

Thus, the angular velocity quaternion in the $(\bar{\bar{X}}, \bar{\bar{Y}}, \bar{\bar{Z}})$ laboratory reference frame is

$$\begin{aligned} \bar{\bar{\omega}} &= (0, \bar{\bar{\omega}}_1, \bar{\bar{\omega}}_2, \bar{\bar{\omega}}_3) \\ &= 2p\frac{dq(t)}{dt}q(t)^*p^* \end{aligned} \tag{106}$$

The inertial angular acceleration quaternion in the (X, Y, Z) reference frame is then

$$\xi = (0, \xi_1, \xi_2, \xi_3)$$

$$= q(t)*p*\frac{d\bar{\omega}}{dt}pq(t)$$

$$= 2\left[q(t)*\frac{d^2q(t)}{dt^2} + q(t)*\frac{dq(t)}{dt}\ \frac{dq(t)}{dt}*q(t)\right] \qquad (107)$$

If $c_i = (0, c_{i1}, c_{i2}, c_{i3})$ is an input axis direction cosine quaternion relative to the (X, Y, Z) frame of an ideal angular accelerometer, then the theoretical value of the output of the instrument is

$$\alpha_i = \sum_{j=1}^{3} \xi_j c_{ij} \text{ radians/s}^2 \qquad (108)$$

Scale factor and bias are ignored because an ideal instrument is assumed. A three-axis angular accelerometer would make three measurements relative to three mutually orthogonal input axes c_1, c_2, c_3 and give complete visibility into the angular acceleration.

5.3 PHOTOGRAPHIC

Triangulation analysis of the film from movie cameras attached to the sled yield coordinates of fiducials relative to the sled frame versus time. The fiducials are attached to the subject at various points, e.g., on the bridge of the nose or beside an eye.

The sled frame coordinates that are given for each fiducial versus time are $(-\bar{X}, \bar{Y}, \bar{Z})$. Note that the photographic data employs a left hand coordinate system, which has to be accounted for when processing observations with the Kalman Filter-Smoother software, which uses the right hand coordinate systems of Figures 3-1 and 3-2 for internal computations.

Let

$z_0 = (0, z_{01}, z_{02}, z_{03})$ = initial sled frame coordinates of the center of the accelerometer array (cm)

$f_{01} = (0, f_{0i1}, f_{0i2}, f_{0i3})$ = initial sled frame coordinates of fiducial i (cm)

The above quantities have to be derived from experimental measurements, which are given in the left hand coordinate system and measured in inches.

Let

$e_i = (0, e_{i1}, e_{i2}, e_{i3})$ = fixed position coordinates of fiducial i relative to the accelerometer array frame (cm)

It is assumed that the fiducials and the accelerometer array are rigidly tied together, which is not strictly true, because

(1) An accelerometer array strapped to the head can move relative to the head during the experiment, although this is less of a problem for an array rigidly attached to the teeth;

(2) The fiducials are attached to the skin, which can deform during the experiment, except that certain areas, such as the bridge of the nose, deform less than others.

If the sled and accelerometer array frames are parallel at the initial time, then

$$e_{ij} = f_{0ij} - z_{0j}, \quad j = 1, 2, 3 \tag{109}$$

If

$q_0 = (q_{01}, q_{02}, q_{03}, q_{04})$

represents an initial quaternion rotation from the accelerometer array frame to the sled frame at the initial time, then

$$e_i = q_0^* (f_{0i} - z_0) q_0 \tag{110}$$

Given the state

$$\vec{x} = (\vec{y}, \vec{z}, \vec{q})$$

at time t, the sled frame coordinates of fiducial i at that time are by Equation (50)

$$f_i = (0, f_{i1}, f_{i2}, f_{i3}) = (0, z_1, z_2, z_3) + qe_iq^* \quad (111)$$

where

$$q = (q_1, \ldots, q_4) \text{ and } e_i = (0, e_{i1}, e_{i2}, e_{i3})$$

Let

$\beta_{i1}, \beta_{i2}, \beta_{i3}$ = theoretical values of fiducial i photographic observables

Then

$$\beta_{i1} = -\lambda_b f_{i1} \quad (112)$$

$$\beta_{i2} = \lambda_b f_{i2} \quad (113)$$

$$\beta_{i3} = \lambda_b f_{i3} \quad (114)$$

where λ_b gives the conversion from centimeters to inches:

$$\lambda_b = 1/2.54 = 0.3937 \quad (115)$$

5.4 TRACK SENSORS

An accelerometer mounted on the sled measures the acceleration γ_1 of the sled relative to the track in g. The theoretical value of this observable is

$$\gamma_1 = \lambda_a y_3 \quad (116)$$

A tachometer attached to a wheel running along the track measures the velocity γ_2 of the sled relative to the track in ft/s. The theoretical value of this observable is

$$\gamma_2 = \lambda_c y_2 \tag{117}$$

where λ_c is the conversion from cm/s to ft/s:

$$\lambda_c = 1/(2.54 \times 12) = 1/30.48 = 0.0328084 \tag{118}$$

5.5 QUATERNION CONSTRAINTS

The quaternion constraints are introduced as errorless artificial observations δ_1, δ_2, δ_3 in order to have the Kalman filter update yield quaternion states which satisfy the constraints. By Equations (54), (55), and (56)

$$\delta_1 = 1 - \sum_{i=1}^{4} q_i^2 \tag{119}$$

$$\delta_2 = \sum_{i=1}^{4} q_i q_{i+4} \tag{120}$$

$$\delta_3 = \sum_{i=1}^{4} q_i q_{i+8} - \sum_{i=1}^{4} q_{i+4}^2 \tag{121}$$

The observed values of these observables are zero with zero error.

SECTION 6

PARTIAL DERIVATIVES OF OBSERVABLES

The partial derivatives of the observables with respect to the states are required to calculate the Kalman filter gain matrix.

6.1 LINEAR ACCELEROMETER ARRAY

Let $(x_1, \ldots, x_{24})$ be given by Equation (62). Differentiation of Equation (101) yields

$$\frac{\partial x_i}{\partial x_\ell} = \lambda_a \sum_{j=1}^{3} \frac{\partial \eta_{ij}}{\partial x_\ell} c_{ij} \tag{122}$$

where the quaternion partial derivatives are

$$\frac{\partial \eta_i}{\partial x_\ell} = \left(0, \frac{\partial \eta_{i1}}{\partial x_\ell}, \frac{\partial \eta_{i2}}{\partial x_\ell}, \frac{\partial \eta_{i3}}{\partial x_\ell}\right) \tag{123}$$

By Equation (100)

$$\frac{\partial \eta_i}{\partial y_\ell} = 0, \quad \ell = 1, 2 \tag{124}$$

$$\frac{\partial \eta_i}{\partial y_3} = q^* p^* (0, 0, -1, 0) pq \tag{125}$$

$$\frac{\partial \eta_i}{\partial z_\ell} = 0, \quad \ell = 1, \ldots, 6 \tag{126}$$

$$\frac{\partial \eta_i}{\partial z_7} = q^* (0, 1, 0, 0) q \tag{127}$$

$$\frac{\partial \eta_i}{\partial z_8} = q^*(0,\ 0,\ 1,\ 0)q \tag{128}$$

$$\frac{\partial \eta_i}{\partial z_9} = q^*(0,\ 0,\ 0,\ 1)q \tag{129}$$

$$\begin{aligned}\frac{\partial \eta_i}{\partial q_\ell} = {} & \frac{\partial q^*}{\partial q_\ell}[(0,\ z_7,\ z_8,\ z_9) + p^*(0,\ 0,\ -y_3,\ q)p]q \\ & + q^*[(0,\ z_7,\ z_8,\ z_9) + p^*(0,\ 0,\ -y_3,\ q)p]\frac{\partial q}{\partial q_\ell} \\ & + \left[\left(\frac{\partial q^*}{\partial q_\ell}\ \frac{d^2q}{dt^2}\right) b_i + b_i\left(\frac{d^2q^*}{dt^2}\ \frac{\partial q}{\partial q_\ell}\right)\right. \\ & + 2\left(\frac{\partial q^*}{\partial q_\ell}\ \frac{dq}{dt}\right) b_i\left(\frac{dq^*}{dt}q\right) \\ & \left. + 2\left(q^*\frac{dq}{dt}\right) b_i\left(\frac{dq^*}{dt}\ \frac{\partial q}{\partial q_\ell}\right)\right], \\ & \ell = 1,\ \ldots,\ 4\end{aligned} \tag{130}$$

$$\begin{aligned}\frac{\partial \eta_i}{\partial q_\ell} = {} & 2\left[\left(q^*\frac{\partial}{\partial q_\ell}\left(\frac{dq}{dt}\right)\right) b_i\left(\frac{dq^*}{dt}q\right)\right. \\ & \left. + \left(q^*\frac{dq}{dt}\right) b_i\left(\frac{\partial}{\partial q_\ell}\left(\frac{dq^*}{dt}\right)q\right)\right], \\ & \ell = 5,\ \ldots,\ 8\end{aligned} \tag{131}$$

$$\begin{aligned}\frac{\partial \eta_i}{\partial q_\ell} = {} & \left[\left(q^*\frac{\partial}{\partial q_\ell}\left(\frac{d^2q}{dt^2}\right)\right) b_i + b_i\left(\frac{\partial}{\partial q_\ell}\left(\frac{d^2q^*}{dt^2}\right)q\right)\right], \\ & \ell = 9,\ \ldots,\ 12\end{aligned} \tag{132}$$

where, for example, $\partial q/\partial q_\ell$ is a quaternion with zero entries except for a 1 at position ℓ.

6.2 IDEAL ANGULAR ACCELEROMETER

Differentiation of Equation (108) yields

$$\frac{\partial \alpha_i}{\partial x_\ell} = \sum_{j=1}^{3} \frac{\partial \xi_j}{\partial x_\ell} c_{ij} \tag{133}$$

where the quaternion partial derivatives are

$$\frac{\partial \xi}{\partial x_\ell} = \left(0, \frac{\partial \xi_1}{\partial x_\ell}, \frac{\partial \xi_2}{\partial x_\ell}, \frac{\partial \xi_3}{\partial x_\ell}\right) \tag{134}$$

By Equation (107)

$$\frac{\partial \xi}{\partial y_\ell} = 0, \quad \ell = 1, 2, 3 \tag{135}$$

$$\frac{\partial \xi}{\partial z_\ell} = 0, \quad \ell = 1, \ldots, 9 \tag{136}$$

$$\frac{\partial \xi}{\partial q_\ell} = 2\left[\frac{\partial q^*}{\partial q_\ell}\frac{d^2 q}{dt} + \frac{\partial q^*}{\partial q_\ell}\frac{dq}{dt}\frac{dq^*}{dt}q + q^*\frac{dq}{dt}\frac{dq^*}{dt}\frac{\partial q}{\partial q_\ell}\right],$$

$$\ell = 1, \ldots, 4 \tag{137}$$

$$\frac{\partial \xi}{\partial q_\ell} = 2\left[q^*\frac{\partial}{\partial q_\ell}\left(\frac{dq}{dt}\right)\frac{dq^*}{dt}q + q^*\frac{dq}{dt}\frac{\partial}{\partial q_\ell}\left(\frac{dq^*}{dt}\right)q\right],$$

$$\ell = 5, \ldots, 8 \tag{138}$$

$$\frac{\partial \xi}{\partial q_\ell} = 2q^*\frac{\partial}{\partial q_\ell}\left(\frac{d^2 q}{dt^2}\right),$$

$$\ell = 9, \ldots, 12 \tag{139}$$

6.3 PHOTOGRAPHIC

Differentiation of Equations (112), (113), and (114) yields

$$\frac{\partial \beta_{i1}}{\partial x_\ell} = -\lambda_b \frac{\partial f_{i1}}{\partial x_\ell} \tag{140}$$

$$\frac{\partial \beta_{i2}}{\partial x_\ell} = \lambda_b \frac{\partial f_{i2}}{\partial x_\ell} \tag{141}$$

$$\frac{\partial \beta_{i3}}{\partial x_\ell} = \lambda_b \frac{\partial f_{i3}}{\partial x_\ell} \tag{142}$$

where the quaternion partial derivatives are

$$\frac{\partial f_i}{\partial x_\ell} = \left(0, \frac{\partial f_{i1}}{\partial x_\ell}, \frac{\partial f_{i2}}{\partial x_\ell}, \frac{\partial f_{i3}}{\partial x_\ell}\right) \tag{143}$$

By Equation (111)

$$\frac{\partial f_i}{\partial y_\ell} = 0, \qquad \ell = 1, 2, 3 \tag{144}$$

$$\frac{\partial f_i}{\partial z_1} = (0, 1, 0, 0) \tag{145}$$

$$\frac{\partial f_i}{\partial z_2} = (0, 0, 1, 0) \tag{146}$$

$$\frac{\partial f_i}{\partial z_3} = (0, 0, 0, 1) \tag{147}$$

$$\frac{\partial f_i}{\partial z_\ell} = 0, \qquad \ell = 4, \ldots, 9 \tag{148}$$

$$\frac{\partial f_i}{\partial q_\ell} = \frac{\partial q}{\partial q_\ell} e_i q^* + q e_i \frac{\partial q^*}{\partial q_\ell}$$

$$\ell = 1, \ldots, 4 \tag{149}$$

$$\frac{\partial f_i}{\partial q_\ell} \qquad \ell = 5, \ldots, 12 \tag{150}$$

6.4 TRACK SENSORS

By Equations (116) and (117)

$$\frac{\partial \gamma_1}{\partial y_3} = \lambda_b \tag{151}$$

$$\frac{\partial \gamma_2}{\partial y_2} = \lambda_c \tag{152}$$

with all other partial derivatives being zero.

6.5 QUATERNION CONSTRAINTS

Differentiation of Equations (119), (120), and (121) yields

$$\frac{\partial \delta_i}{\partial y_\ell} = 0, \qquad i = 1, 2, 3; \quad \ell = 1, 2, 3 \tag{153}$$

$$\frac{\partial \delta_i}{\partial z_\ell} = 0, \qquad i = 1, 2, 3; \quad \ell = 1, \ldots, 9 \tag{154}$$

$$\frac{\partial \delta_1}{\partial q_\ell} = -2q_\ell, \qquad \ell = 1, \ldots, 4 \tag{155}$$

$$\frac{\partial \delta_1}{\partial q_\ell} = 0, \qquad \ell = 5, \ldots, 12 \tag{156}$$

$$\frac{\partial \delta_2}{\partial q_\ell} = q_{\ell+4} \qquad \ell = 1, \ldots, 4 \tag{157}$$

$$\frac{\partial \delta_2}{\partial q_\ell} = q_{\ell-4}, \qquad \ell = 5, \ldots, 8 \tag{158}$$

$$\frac{\partial \delta_2}{\partial q_\ell} = 0, \qquad \ell = 9, \ldots, 12 \tag{159}$$

$$\frac{\partial \delta_3}{\partial q_\ell} = q_{\ell+8}, \qquad \ell = 1, \ldots, 4 \tag{160}$$

$$\frac{\partial \delta_3}{\partial q_\ell} = -2q_\ell, \qquad \ell = 5, \ldots, 8 \tag{161}$$

$$\frac{\partial \delta_3}{\partial q_\ell} = q_{\ell+8}, \qquad \ell = 9, \ldots, 12 \tag{162}$$

6.6 CHECK OF PARTIAL DERIVATIVES

The coding of the observable partial derivatives can be checked by the difference method. Namely, given a state vector

$$\vec{x} = (x_1, \ldots, x_{24}),$$

the theoretical value of observable $s_i(\vec{x})$ is computed and also $\partial s_i/\partial x_j$. The state vector is changed by the increment

$$\vec{\Delta}_j = (0, \ldots, 0, \Delta_j, 0, \ldots, 0) \tag{163}$$

$$\vec{x} + \vec{\Delta j} = (x, \ldots, x_{j-1}, x_j + \Delta_j, x_{j+1}, \ldots, x_{24}) \tag{164}$$

Then it is checked that

$$\frac{1}{2}\left[\frac{\partial s_i(\vec{x} + \vec{\Delta}_j)}{\partial x_j} + \frac{s_i(\vec{x})}{\partial x_j}\right]$$

$$= \frac{s_i(\vec{x} + \vec{\Delta}_j) - s_i(\vec{x})}{\Delta_j} \tag{165}$$

The coding of the partial derivatives of normalized quaternion components with respect to unnormalized quaternion components and the partial derivatives of the state components at time t_{k+1} with respect to those at time t_k can also be checked by this method.

SECTION 7

KALMAN FILTER AND SMOOTHER

Let the state vector

$$\vec{x} = (x_1, \ldots x_{24})^T \tag{166}$$

be defined by Equation (62), where the superscript T denotes transpose changing the row vector in a column vector. Let the state transition from time t_k to t_{k+1} be

$$\vec{x}(t_{k+1}|t_k) = \vec{F}(\vec{x}(t_k)) + \vec{W}(t_{k+1}, t_k)$$

$$k = 0, 1, \ldots, N \tag{167}$$

where $\vec{W}$ is the integral of the zero mean Gaussian white noise process $\vec{w}$, so that

$$E(\vec{W}) = 0 \tag{168}$$

where E denotes expectation (see Section 7.4). Let

$Q(t_{k+1}, t_k)$ = covariance matrix of $\vec{W}(t_{k+1}, t_k)$ so that

$$Q_{ij} = E(W_i W_j), \qquad i, j = 1, \ldots, 24 \tag{169}$$

Let the observable vector be

$$\vec{s}(t_k) = (\alpha_1, \ldots, \alpha_a, \beta_1, \ldots, \beta_b, \gamma_1, \gamma_2, \delta_1, \delta_2, \delta_3)^T \tag{170}$$

where its length can vary at different observable times. The observables in terms of the states are

$$\vec{s}(t_{k+1}) = \vec{H}(\vec{x}(t_{k+1})) + \vec{r}_{k+1} \tag{171}$$

where $\vec{r}_{k+1}$ is zero mean Gaussian noise with covariance matrix R_{k+1}, uncorrelated from one observing time to the next. It can be taken as a diagonal matrix with elements that represent the squares of standard deviations of the observable measurements. These standard deviations are zero for the quaternion constraint observables δ_1, δ_2, δ_3.

Formulas are now given for forward and backward extended Kalman filters and for the Kalman smoother which is the optimal combination of the two filters[2].

7.1 FORWARD FILTER

At the initial time t_0, the state initial condition for the forward filter $\vec{x}_f(t_0)$ is specified by, e.g., Equations (49), (51), and (52) with velocities and accelerations zero for an experiment with the sled initially at rest. The covariance $P_f(t_0)$ of the initial state also has to be specified. It can be taken to be a diagonal matrix with elements that represent the squares of the standard deviations of the uncertainty of the initial conditions.

The expected value of the state $x_f(t_{k+1}|t_k)$ at time t_{k+1} given the state $x_f(t_k)$ at time t_k is calculated from Equation (167) with $\vec{w} = \vec{0}$ in the form of Equations (57) through (60). The state transition Jacobian matrix

$$J_{k+1} = \frac{\partial \vec{x}_f(t_{k+1}|t_k)}{\partial \vec{x}_f(t_k)} = \left[\frac{\partial x_{fi}(t_{h+1}|t_k)}{\partial x_{fj}(t_k)}\right] \tag{172}$$

is calculated from Equations (71) through (80) and (91). For the first 12 linear state variables it is the matrix exponential state transition matrix. For the last 12 state variables the matrix exponential is modified by the partial derivatives of the nonlinear quaternion constraints, which, however, are assumed to form the identity matrix.

The state covariance matrix $P_f(t_{k+1}|t_k)$ at time t_{k+1} given the covariance $P_f(t_k)$ at time t_k and the covariance $Q(t_{k+1}, t_k)$ of the dynamical noise is[2]

$$P_f(t_{k+1}|t_k) = J_{k+1}P_f(t_k)J_{k+1}^T + Q(t_{k+1}, t_k) \tag{173}$$

where J^T is the transpose of J.

The theoretical values of the observables $\vec{H}$ are calculated from Equations (100) through (121). The observables Jacobian matrix

$$L_{k+1} = \frac{\partial \vec{H}(\vec{x}_f(t_{k+1}|t_k))}{\partial \vec{x}_f(t_{k+1}|t_k)} \tag{174}$$

is calculated from Equations (122) through (162).

The Kalman filter gain matrix is[2]

$$K_{k+1} = P_f(t_{k+1}|t_k)L_{k+1}^T \left[L_{k+1}P_f(t_{k+1}|t_k)L_{k+1}^T + R_{k+1}\right]^{-1} \tag{175}$$

Note that this form of the gain matrix allows zero rows and columns in R, as is the case when the perfect quaternion constraint observables are included. However, the total matrix in the brackets [] has to be invertable.

It is possible that for multiple observations at a given time some combinations of the observables would be essentially equivalent, which might cause noninvertability of the LP_fL^T portion of the matrix in the brackets []. However, the nonzero portion of the observation error matrix R will likely make the sum in brackets [] invertable. If not, observations at a given time can be passed through the Kalman filter sequentially along with the 3 quaternion constraint observables. In this manner, complete processing of n observations at a given time would involve n inversions of 4x4 matrices, instead of one inversion of an (n+3)x(n+3) matrix.

If the data acquisition system makes the A/D conversion measurements at distinct times, rather than using a sample and hold to obtain everything at the same time, then this sequential processing would have to be done anyway.

The expected value of the state $x_f(t_{k+1})$ at time t_{k+1} given the state at time t_k and the observables at time t_{k+1} is[2]

$$\vec{x}_f(t_{k+1}) = \vec{x}_f(t_{k+1}|t_k) + K_{k+1}\,[\vec{s}(t_{k+1}) - \vec{H}(\vec{x}_f(t_{k+1}|t_k))] \tag{176}$$

The covariance $P_f(t_k + 1)$ of the state at time t_{k+1} given the state at time t_k and the observables at time t_{k+1} is[2]

$$P_f(t_{k+1}) = [I - K_{k+1}L_{k+1}]P_f(t_{k+1}|t_k)$$

where I is the identity matrix.

The above formulas define the extended Kalman forward filter with the nominal trajectory for the extended filter linearization being updated each observation point. Extended rather than linear Kalman filtering is required because of the nonlinearities in the quaternion constraints and in the formulas for the observables in terms of the states.

The quaternion constraint information appears implicitly in the Kalman update Equation (176), because the constraints are taken to be perfect observations. However, the linearization employed in extended Kalman filtering could yield an update $(x_1(t_{k+1}), \ldots, x_{24}(t_{k+1}))$ for which constraints are not satisfied by the quaternion part $(x_{13}(t_{k+1}), \ldots, x_{24}(t_{k+1}))$. Therefore, the normalization Equations (58), (59), and (60) should be applied. Let $\vec{\bar{x}}$, $\bar{P}$ be the state and its covariance matrix before the quaternion normalization and let $\vec{x}$, P these quantities after the quaternion normalization at time t_{k+1}. Then

$$P = \left(\frac{\partial \vec{x}}{\partial \vec{x}}\right) \bar{P} \left(\frac{\partial \vec{x}}{\partial \vec{x}}\right)^T \tag{178}$$

where

$$\frac{\partial \vec{x}}{\partial \vec{x}} = \begin{bmatrix} I_{12x12} & 0_{12x12} \\ 0_{12x12} & \frac{\partial q}{\partial \bar{q}} \end{bmatrix} \tag{179}$$

with the 12x12 matrix $(\partial q/\partial \bar{q})$ being given by the Equation (91) identity matrix, for the reasons given at the end of Section 4.2.

7.2 BACKWARD FILTER

At the last time point t_n in the data, let

$$\vec{x}_b(t_n) = \vec{x}_f(t_n) \tag{180}$$

The covariance of this initial value for the backward Kalman filter is

$$P_b(t_n) = \infty, \qquad P_b(t_n)^{-1} = 0 \tag{181}$$

since the Kalman smoother state is the optimal combination of the forward and backward Kalman filter states weighted by P_f^{-1} and P_b^{-1}, and the Kalman smoother state has to equal the forward Kalman filter state at time t_n, where both contain all the observable information from time t_0 to time t_n.

The expected value of the state $\vec{x}_b(t_{k-1}|t_k)$ at time t_{k-1} given the state $x_b(t_k)$ at time t_k is calculated from Equations (57) through (60) with t_{k+1} replaced by t_{k-1}, so that $(t_{k-1} - t_k)$ is negative. The state Jacobian matrix

$$J_{k-1} = \frac{\partial \vec{x}_b(t_{k-1}|t_k)}{\partial \vec{x}_b(t_k)} \tag{182}$$

is calculated from Equations (71) through (80) and (91).

The state covariance matrix $P_b(t_{t-1}|t_k)$ at time t_{k-1} given the covariance $P_b(t_k)$ at time t_k and the covariance $Q(t_{k-1}, t_k)$ of the dynamical noise (same in the backward and forward directions) is[2]

$$P_b(t_{k-1}|t_k) = J_{k-1}P_k(t_b)J_{k-1}^T + Q(t_{k-1}, t_k) \tag{183}$$

For $k = N$, $P_b(t_N) = \infty$, which implies that $P_b(t_{k-1}|t_k) = \infty$.

The theoretical values of the observables H is calculated from Equations (100) through (121). The observable Jacobian matrix

$$L_{k-1} = \frac{\partial \vec{H}(\vec{x}_b(t_{k-1}|t_k))}{\partial \vec{x}_b(t_{k-1}|t_k)} \tag{184}$$

is calculated from Equations (122) through (162).

The Kalman filter gain matrix is[2]

$$K_{k-1} = P_b(t_{k-1}|t_k)L_{k-1}^T[L_{k-1}P_b(t_{k-1}|t_k)L_{k-1}^T + R_{k-1}]^{-1} \tag{185}$$

The expected value of the state $x_b(t_{k-1})$ at time t_{k-1} given the state at time t_k and the observables at time t_{k-1} is[2]

$$x_b(t_{k-1}) = x_b(t_{k-1}|t_k) + K_{k-1}[s(t_{k-1}) - H(x_b(t_{k-1}|t_k))] \tag{186}$$

The covariance $P_b(t_{k-1})$ of the state at time t_{k-1} given the state at time t_k and the observables at time t_{k-1} is[2]

$$P_b(t_{k-1}) = [I - K_{k-1}L_{k-1}]P_b(t_{k-1}|t_k) \tag{187}$$

These forms of the Kalman filter equations are ideal with the perfect quaternion constraint observables for all except the first step in the backward filter process.

To go from time t_N to t_{N-1} with $P_b(t_N) = \infty$, the following alternative form of the Kalman filter formulas can be used[2]:

$$P_b(t_{k-1})^{-1} = P_b(t_{k-1}|t_k)^{-1} + L_{k-1}^T R_{k-1}^{-1} L_{k-1} \tag{188}$$

$$K_{k-1} = P_b(t_{k-1}) L_{k-1}^T R_{k-1}^{-1} \tag{189}$$

where $P_b(t_{N-1}|t_N)^{-1} = 0$. However, the matrix $L_{N-1}^T R_{N-1}^{-1} L_{N-1}$ can be singular because certain states might not be directly observable from the given measurements at time t_{N-1}. Thus, $P_b(t_{N-1}|t_N)^{-1}$ can be taken as a diagonal matrix with very small diagonal entries. The covariance for the quaternion constraint observables should also be small but nonzero so that R_{N-1}^{-1} exists.

It turns out that for the impact experiments investigated in this report, the backward filter step from time t_N to t_{N-1} could not meaningfully be made, neither with small nonzero entries in $P_b(t_{N-1}|t_N)^{-1}$ and R_{N-1}^{-1} Equations (188) and (189), nor with large but less than infinite entries in $P_b(t_N)$ in Equations (185) and (187). The forward filter worked well because it started from known initial conditions at time t_0. In retrospect it is clear that the backward filter cannot be employed starting with complete uncertainty at time t_N unless the measurements at time t_{N-1} give complete observability into the states. In this situation it is better to smooth the observables before passing them through the Kalman forward filter rather than using an optimal combination of the forward and backward Kalman filters to smooth the states.

If the backward filter were employed, the quaternion normalization described at the end of Section 7.1 should be applied to $x_b(t_{k-1})$ and then the smoother formulas of Section 7.3 utilized.

7.3 SMOOTHER

If both the forward and backward Kalman filters are run, the Kalman smoother state estimate is the following optimal combination of the two filter estimates[2]:

$$P^{-1} = P_f^{-1} + P_b^{-1} \tag{190}$$

$$\vec{x} = P[P_f^{-1} \vec{x}_f + P_b^{-1} \vec{x}_b] \tag{191}$$

where the equations are evaluated for any time t ($t_0 \leq t \leq t_N$) with nonsubscripted quantities being the smoother results.

Because the quaternion constraints are nonlinear, $\vec{x}$ no longer satisfies those constraints exactly even though $\vec{x}_f$ and $\vec{x}_b$ do. Therefore, the normalization of $\vec{x}$ and the updating of P must be performed as described at the end of Section 7.1.

7.4 PLANT NOISE

Successful application of the algorithms described above requires a choise of Q which allows for the unknown but bounded variability in jerk (= change in acceleration), yet optimally combines the information contained in the observables at a given time with the information contained in past states (and also future states if a smoother could be employed).

Suppose in a given impact experiment the observations are uniformly one millisecond apart. Suppose the acceleration level of the order of 10g could change by up to 0.5g in a millisecond. Then the standard deviations of the variability in the state in one millisecond are

acceleration:	500 cm/s^2
velocity:	0.5 cm/s
position:	0.5×10^{-3} cm

The squares of these values can be taken as the covariances in the diagonal $Q(t_k, t_{k+1})$ matrix, except that the small uncertainty in the position covariance could be increased somewhat to account for other sources of uncertainty besides integrated acceleration uncertainty. However, the propogated state uncertainty will likely give appropriate magnitudes for the uncertainties in position and velocity for closely spaced observations.

For the quaternion rotation uncertainties, appropriate standard deviations for changes in one millisecond could be

angular acceleration:	10 rad/s^2
angular velocity:	10^{-2} rad/s
angular position:	10^{-5} rad

for the impact experiments of concern in this report.

7.5 MATRIX MANIPULATION

Symmetric covariance matrices should be calculated and stored in the computer in lower diagonal form. That is, a symmetrix matrix S is stored in a vector array as

$$S(J, K) = \begin{cases} S(J + (K(K-1))/2), & J \leq K \\ S(K + (J(J-1))/2), & K \leq J \end{cases} \quad (192)$$

The usual Fortran storage assignment for a general NXN matrix M is

$$M(J, K) = M(J + (K-1)N) \quad (193)$$

Subroutines are required to multiply a symmetric matrix by a nonsymmetric matrix (MS or SM) to get a nonsymmetric results, to compute MSM^T to get a symmetric result, and to multiply general matrices.

The computer subroutine to calculate the inverse of a symmetric matrix stored in lower diagonal form by the Gauss-Jordan direct method should choose all the pivot elements on the diagonal, so no interchange of rows or columns is necessary.

There can be numerical problems with matrix entries being badly out of scale relative to one another, especially with matrix inversion. Clever choice of units could help mitigate the problem. However, it is easier to choose convenient units (cm, s, g, etc.) and then use automatic scaling before performing a matrix inversion. Namely, let $S = (S_{jk})$ be a symmetric matrix. Define a diagonal matrix $D = (D_{jk})$ with diagonal entries

$$D_{jj} = 1/\sqrt{S_{jj}} \tag{194}$$

where the diagonal elements of S are no doubt positive because it is probably a covariance or related matrix. Define a new symmetric matrix

$$U = DSD \tag{195}$$

The diagonal elements of U are 1, and those off the diagonal are likely not way out of scale, so that it is numerically easier to invert. Then the inverse of S is

$$S^{-1} = DU^{-1}D \tag{196}$$

SECTION 8
DATA ANALYSIS

Two lateral and two fore-aft (eyes out) impact sled tests were analyzed with the software written using the formulas presented in this report. One experiment of a given type involved a dummy subject and the other a living human subject. A nine-accelerometer array (9-TAP) using Endevco 2264-200 piezoresistive accelerometers was strapped to the right side of the subject's head for the lateral impact tests, and a similar three-accelerometer array was used for the fore-aft impact tests. The piezoresistive accelerometer voltage outputs were converted to g units using precalibrated scale factors. Biases were determined from the first few data points in each experiment when the subject was stationary before the impact event.

Head fiducials were tracked by motion picture cameras. Triangulation gave the sled fiducials as a function of time in inches. The acceleration and velocity of the sled relative to the track were measured in g and ft/s, respectively.

As the sled accelerated down the track away from its rest position under the impetus provided by a piston, the subject's constrained yielding torso was dragged along, as was the subject's head attached to the torso by the neck. The problem is to derive the motion of the head (translational and angular position, velocity, and acceration) by processing all the data simultaneously through the Kalman filter.

The nominal error standard deviations assumed for the experimental measurements are listed in Table 8-1. The observation covariance matrix R is diagonal with diagonal elements the squares of the standard deviations. Each observable has its own units. The theoretical values of the observables in the units internal to the software (cm and s) are converted to the observable units by multiplying by the appropriate factors.

Table 8-1. Measurement standard deviations.

OBSERVABLE TYPE	STANDARD DEVIATION
Linear Piezoresistive Accelerometer	0.1 g
Photographic	0.1 inch
Track Velocity	0.1 ft/s
Track Acceleration	0.1 g

The interval between accelerometer measurements is one millisecond, whereas photographic measurements are two milliseconds apart. An impact event lasts about 0.3 seconds. The Kalman filter allows different numbers of observables at each one millisecond time point, with the state being propagated between time points by the dynamical equations. The dynamical noise Q chosen in Section 7.4 for these experiments allows the proper weighting of present observable information relative to the past observable and initial condition information contained in the propagated state variables.

8.1 LATERAL IMPACT TESTS

A diagram of the 9-TAP is given in Figure 8-1. The right-hand coordinate convention of the software is employed rather than the left-hand convention of the experiment.

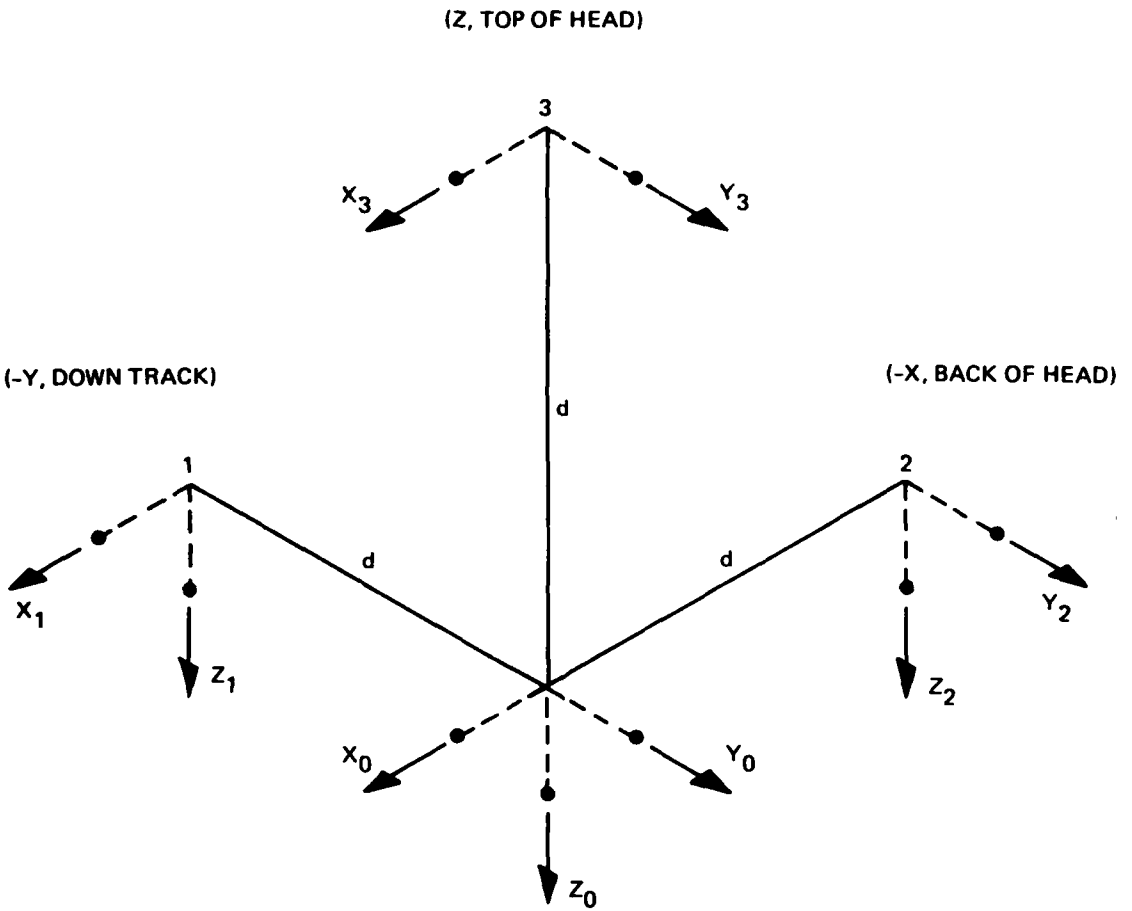

Figure 8-1. Nine accelerometer array orientation.

There are three accelerometers near the origin 0 of the 9-TAP with input axes along the three coordinate axes as shown. At a distance d = 1.5 inches = 3.81 cm along each of the three coordinate axes are two accelerometers with input axes perpendicular to the given axis.

The seismic mass coordinates and input axis directions of the accelerometers relative to the accelerometer array frame are given in Table 8-2. They are offset a distance d' = 0.34 inch = 0.6 cm from the center lines of the array arms.

Table 8-2. Nine accelerometer array coordinates.

d = length of array arms
= 1.5 inches = 3.81 cm
d' = offset of seismic masses from center line of arms
= 0.34 inch = 0.86 cm

ACCELEROMETER		POSITION IN ARRAY			INPUT AXIS DIRECTION COSINES			INITIAL OUTPUT WITHOUT BIAS
Number	Name	b_1	b_2	b_3	c_1	c_2	c_3	
1	X_0	d'	0	0	1	0	0	0
2	Y_0	0	d'	0	0	1	0	0
3	Z_0	0	0	-d'	0	0	-1	-1 g
4	X_1	d'	-d'	0	1	0	0	0
5	Z_1	0	-d	-d'	0	0	-1	-1 g
6	Y_2	-d	d'	0	0	1	0	0
7	Z_2	-d	0	-d'	0	0	-1	-1 g
8	X_3	d'	0	d	1	0	0	0
9	Y_3	0	d'	d	0	1	0	0

At the initial time $t_0 = 0$, the sled is at rest with zero velocities and accelerations. The track, sled, and accelerometer array coordinate axes are all initially parallel with zero relative velocity and acceleration. The origin of the sled frame coordinates and the position of the

accelermeter array frame relative to it vary with each experiment. The origins of the sled and track frames are assumed to coincide at the initial time.

8.1.1 Dummy Test 1363

Lateral impact dummy sled test 1363 is depicted in Figure 8-2. The sled frame has origin in the seat, and the initial position of the center of the nine-accelerometer array and the photographic fiducials relative to the sled frame are given in Table 8-3.

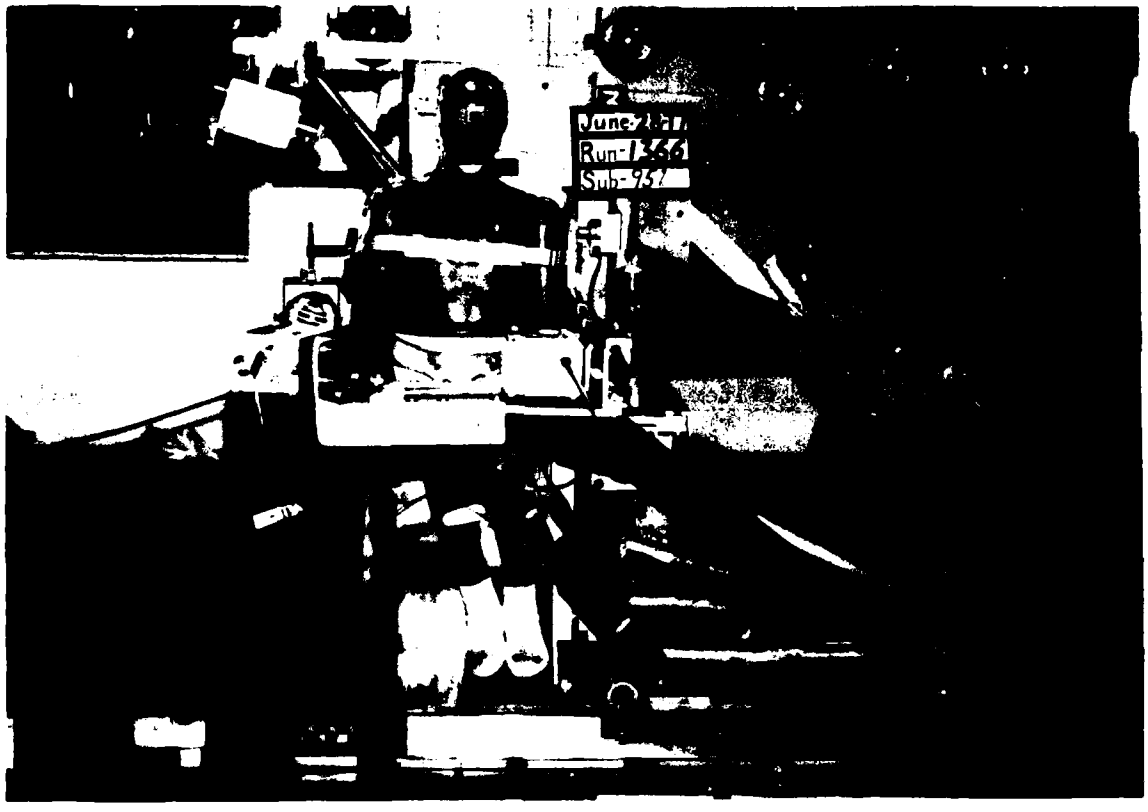

Figure 8-2. Lateral impact dummy sled test 1363.

Table 8-3. Dummy lateral impact test 1363 initial accelerometer array and photographic fiducial coordinates relative to the sled frame*.

	INCHES			CENTIMETERS		
	$\bar{X}$	$\bar{Y}$	$\bar{Z}$	$\bar{X}$	$\bar{Y}$	$\bar{Z}$
9-TAP (z_{10}, z_{20}, z_{30})	8.50	-2.15	34.80	21.59	-5.46	88.39
Right Eye Fiducial (f_{011}, f_{012}, f_{013})	9.00	-0.65	32.55	22.86	-1.65	82.65
Nose Fiducial (f_{041}, f_{042}, f_{043})	10.05	1.60	32.15	25.53	4.06	81.66

Typical accelerometer and photographic observables and Kalman filter post-fit residuals are given in Figures 8-3 and 8-4. The residuals result from the Kalman filter trying to best fit the data from the nine-accelerometer array, the sled accelerometer and velocity tachometer, and the three coordinates of each of the two photographic fiducials.

The Kalman filter is threading the states through the observables, but the residuals are not as small as might be desired. For accelerometer readings of over 10 g, the residuals were between -2.5 and +1.8 g. The photographic fiducial residuals were between -1.0 and +1.2 inches. The sled acceleration and velocity relative to the track had 0.2 g and 0.5 ft/s maximum magnitude residuals.

The dummy had a three-accelerometer array at the center of its head. The residuals were as large as 22 g in magnitude. The most probable cause of these discrepencies is some error in the input coordinates to the software.

---

*Right-handed coordinate frame, so that $\bar{X}$ is the negative of the value in the left-hand photographic measurement frame.

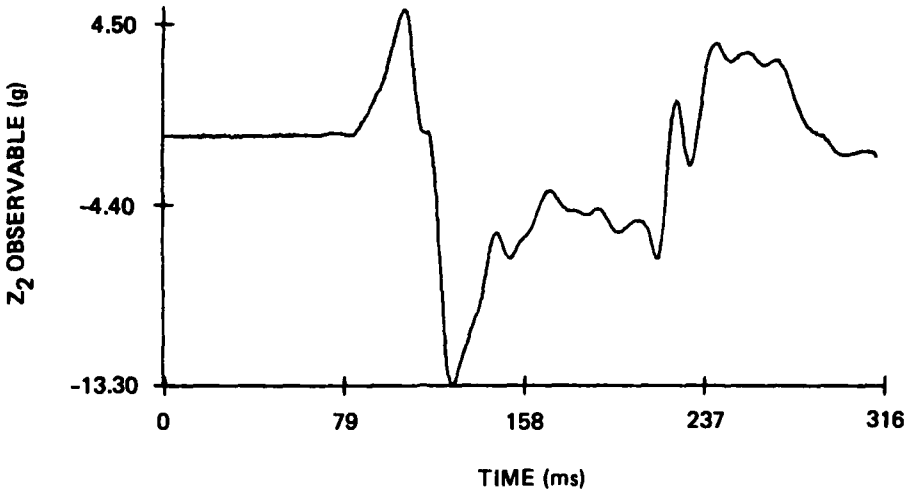

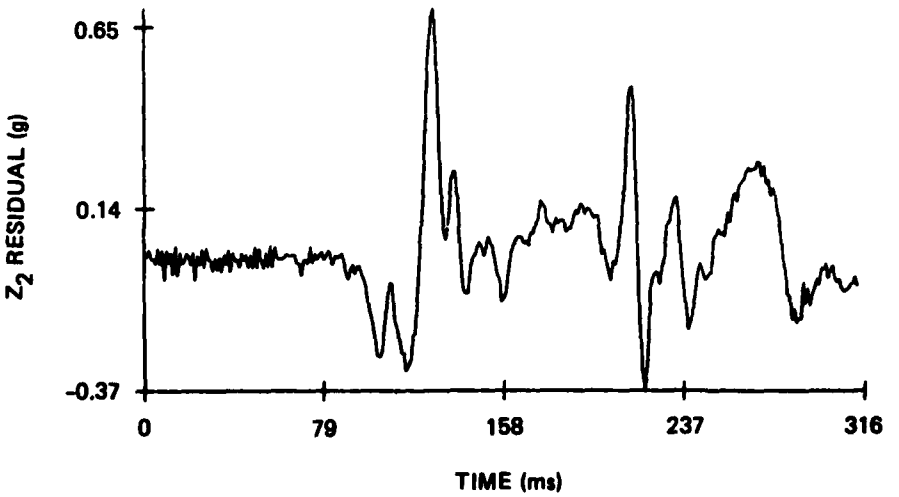

Figure 8-3. Dummy test 1363 accelerometer Z_2 observable and residual.

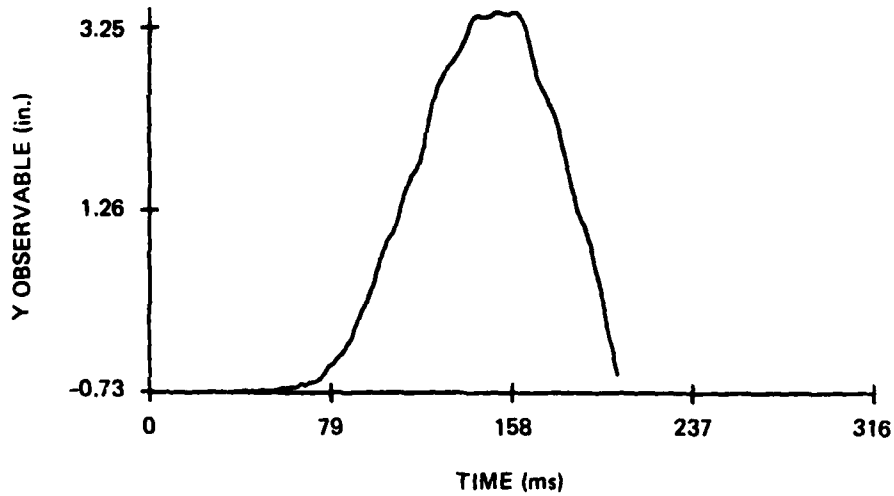

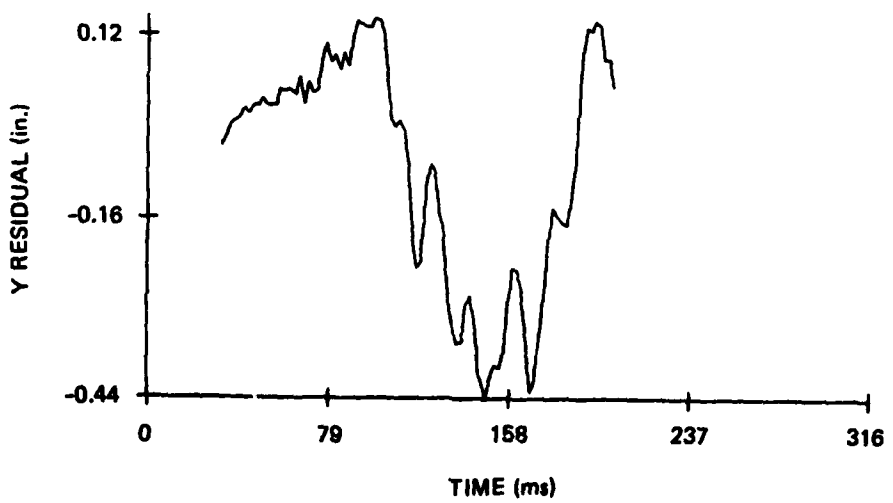

Figure 8-4. Dummy test 1363 right eye fiducial Y observable and residual.

8.1.2 Human Test 1313

Lateral impact human sled test 1313 is similar to the dummy test discussed in Section 8.1.1. The initial position of the center of the nine-accelerometer array and the photographic fiducials relative to the sled frame are given in Table 8-4. The Kalman filter was again obviously tracking the observables, but one of the accelerometer residuals got as large as -3.3 g and another was as large as +2.8 g for accelerometer measurements of the order of 10 g.

Table 8-4. Human lateral impact test 1313 initial accelerometer array and photographic fiducial coordinates relative to the sled frame*.

	INCHES			CENTIMETERS		
	$\bar{X}$	$\bar{Y}$	$\bar{Z}$	$\bar{X}$	$\bar{Y}$	$\bar{Z}$
9-TAP (z_{10}, z_{20}, z_{30})	6.42	-1.94	32.24	16.31	-4.93	81.89
Right Eye Fiducial (f_{011}, f_{012}, f_{013})	7.54	-0.31	31.92	19.15	-0.79	81.08
Nose Fiducial (f_{041}, f_{042}, f_{043})	8.80	2.08	32.75	22.35	5.28	83.19

8.2 FORE-AFT (EYES OUT) IMPACT TESTS

Data from fore-aft (eyes out) impact sled tests 1133 (human) and 1229 (dummy) were analyzed. There was a nine-accelerometer array strapped to the subject's forehead. In order to simulate the situation of a three-accelerometer array afixed to the teeth inside the mouth, only three of the nine outputs were obtained for use in the analysis.

*Right-handed coordinate frames, so that $\bar{X}$ is the negative of the value in the left-hand photographic measurement frame.

There was photographic fiducial data from two head fiducials in each experiment. Only the X and Z coordinates versus time were recorded, since the motion of the subject was mainly in the (X, Z) impact plane. Therefore, in the Kalman filter analysis the Y accelerometer output was ignored, and only the X and Z accelerometer data used along with the X and Z photographic fiducial data.

In both experiments, the Kalman filter tracked the observables until the start of the impact event, at which point the Kalman filter diverged from the observables, with some residuals being greater than 10^3 g. The cause of this divergence requires further investigation.

8.3 ANGULAR ACCELEROMETER COVARIANCE ANALYSIS

The Kalman filter software has the option of reading a trajectory output tape from a previous Kalman filter fit, adding dummy observations, and calculating the state covariance of the input trajectory for the expanded observation set. The Kalman filter propagation of the trajectory is skipped and the input trajectory states are unchanged with only the state covariance being updated.

The output magnetic tape from lateral impact experiment 1363 was read and a covariance analysis performed with the addition of ideal angular accelerometer observables in three orthogonal directions. The angular accelerometer measurement error was assumed to be 0.01 rad/s^2. The quaternion acceleration covariance improved by almost an order of magnitude versus not having the angular accelerometer observables. The quaternion velocity and position covariance improved by 20 percent and less than 10 percent respectively.

The covariance analysis assumed that the measurements are without bias, including dimensional errors and cross axis sensitivities in the accelerometer array. The real advantage of an angular accelerometer would be to counteract the effect of such biases in the piezoresistive accelerometer array. To obtain the true effect of the new observable on the state covariance, bias states would have to be added to the Kalman filter and their uncertainty included in the covariance calculations.

REFERENCES

1. P. DuVal, Homographies, Quaternions and Rotations, Clarendon Press, Oxford, England, 1964, Chapter 3.

2. A. Gelb, Applied Optimal Estimation, The MIT Press, Cambridge, Massachusetts, 1974.

*U.S.Government Printing Office: 1983 — 659-005/2042


MEI
8